Clinical Neurophysiology 164 (2024) 1–18

Contents lists available at ScienceDirect

Clinical Neurophysiology

journal homepage: www.elsevier.com/locate/clinph

Review

Muscle excitability testing

H. Tankisi [a,b,*], H. Bostock [c], S.V. Tan [c,d], J. Howells [e], K. Ng [f,g], W.J. Z'Graggen [h]

[a] Department of Clinical Neurophysiology, Aarhus University Hospital, Aarhus, Denmark
[b] Institute of Clinical Medicine, Aarhus University Hospital, Aarhus, Denmark
[c] Department of Neuromuscular Diseases, UCL Queen Square Institute of Neurology, Queen Square, WC1N 3BG London, United Kingdom
[d] Department of Neurology and Neurophysiology, Guys and St Thomas' NHS Foundation Trust, London, United Kingdom
[e] Central Clinical School, Faculty of Medicine and Health, University of Sydney, Sydney, Australia
[f] Department of Neurology and Neurophysiology, Royal North Shore Hospital, St Leonards, NSW, Australia
[g] University of Sydney, Camperdown, NSW, Australia
[h] Departments Neurology and Neurosurgery, Inselspital, Bern University Hospital, University of Bern, Bern, Switzerland

HIGHLIGHTS

- Muscle excitability testing is a technique that provides *in vivo* information about membrane potential and ion channel function.
- Multi-fibre muscle velocity recovery cycles, frequency ramp and repetitive stimulation protocols are automated and fast methods.
- Muscle excitability testing is used mainly in research but it may have diagnostic uses, particularly in muscle channelopathies.

ARTICLE INFO

Article history:
Accepted 22 April 2024
Available online 07 May 2024

Keywords:
Muscle excitability testing
Muscle velocity recovery cycles
Frequency ramp
Repetitive stimulation
Muscle channelopathies
Myopathy

ABSTRACT

Conventional electrophysiological methods, i.e. nerve conduction studies and electromyography are suitable methods for the diagnosis of neuromuscular disorders, however, they provide limited information about muscle fibre membrane properties and underlying disease mechanisms. Muscle excitability testing is a technique that provides *in vivo* information about muscle fibre membrane properties such as membrane potential and ion channel function.

Since the 1960s, various methodologies have been suggested to examine muscle membrane properties but technical difficulties have limited its use. In 2009, an automated, fast and simple application, the so-called multi-fibre muscle velocity recovery cycles (MVRC) has accelerated the use of muscle excitability testing. Later, frequency ramp and repetitive stimulation protocols have been developed. Though this method has been used mainly in research for revealing disease mechanisms across a broad range of neuromuscular disorders, it may have additional diagnostic uses; value has been shown particularly in muscle channelopathies.

This review will provide a description of the state-of-the art of methodological and clinical studies for muscle excitability testing.

Contents

* Corresponding author at: Department of Clinical Neurophysiology, Aarhus University Hospital, Aarhus, Denmark.
E-mail addresses: hatitank@rm.dk, hatice.tankisi@clin.au.dk (H. Tankisi).

https://doi.org/10.1016/j.clinph.2024.04.022
1388-2457/

1. History of measuring muscle membrane potential and muscle velocity recovery function in human

Electrophysiological examinations of human muscle membranes *in vivo* have focussed on the nature of muscle fibre discharges, propagation velocity and membrane potential. Denslow and Hassett (1943) made recordings of human muscle *in vivo* using needle electrodes to examine motor unit waveforms and their propagation velocity. Beránek recorded resting membrane and action potentials in muscle fibres *in vivo* using a glass micropipette inside an intramuscular syringe mounted on a micrometer, which he carefully advanced into a muscle fibre (Beránek, 1964). This technique was used by Cunningham et al. (1971) in normal subjects and patients with severe debilitating disorders. Special attention was paid to stabilizing the leg and electrode manipulator, and the whole recording was made inside a Faraday cage (see Fig. 1; Cunningham et al., 1971). Cunningham and colleagues found that they were able to reliably record resting membrane potential in all subjects and there was little difference between control subjects and mildly ill patients (mean [SD]: −88.8 [3.8] mV, −89.8 [2.1], respectively). However, the resting membrane potential (RMP) of severely ill patients was markedly depolarized (−66.3 [9.0] mV).

Stålberg found that propagation velocity in human muscle fibres depended on the interval from the preceding discharge, which he termed the Velocity Recovery Function (Stålberg, 1966). In later studies, his group stimulated single muscle fibres with

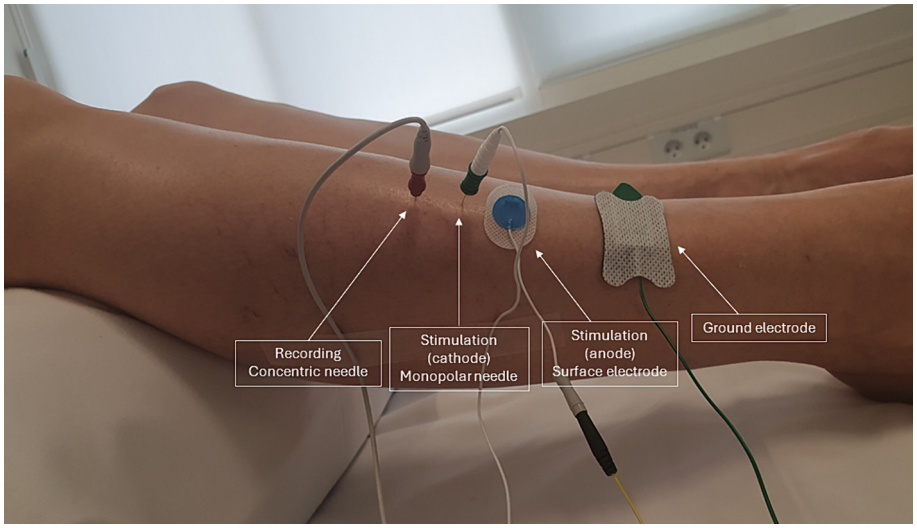

Fig. 1. Electrode arrangement for measurement of muscle VRCs. The cathode (monopolar needle electrode) was inserted perpendicularly into the tibialis anterior muscle. The anode (surface electrode) was placed about 1 cm distal to the cathode. Recordings were made with concentric EMG electrodes introduced into the muscle about 20 mm proximal to the cathode.

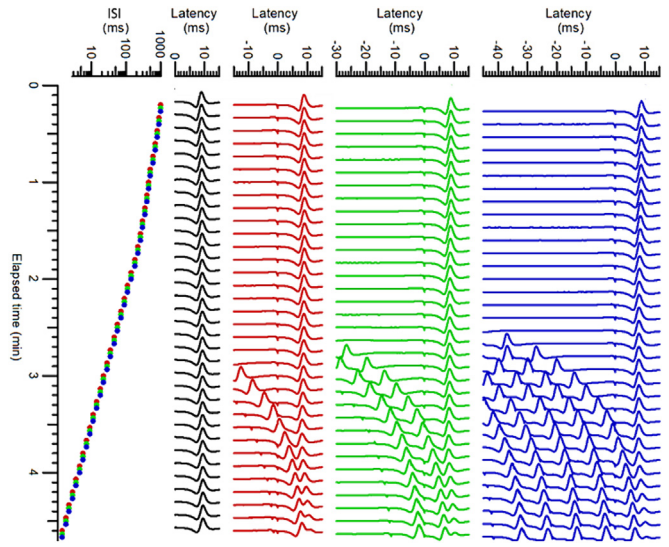

Fig. 2. A recording of MVRCs with test-alone stimuli (black) and 1 (red), 2 (green) and 5 (blue) conditioning stimuli in a healthy control subject, showing interstimulus intervals (ISI) reducing from 1000 to 2 ms over a 5-minute period. Only the last parts of each sweep are illustrated. (For interpretation of the references to colour in this figure legend, the reader is referred to the web version of this article.)

paired electrical stimuli to measure the velocity recovery function in detail (Mihelin et al., 1991). They noted that finding the recording site for a single responding muscle fibre was "often difficult". Nonetheless, they were able to record velocity recovery functions (see Figs. 2 and 3 in Mihelin et al., 1991) which are similar to the velocity recovery cycles in this review.

Allen et al. (2008) assessed muscle-fibre conduction velocities in patients with critical illness myopathy using paired-pulses of 2 to 20 ms in the tibialis anterior muscles and found delayed and dispersed responses and longer absolute refractory period when compared to healthy controls.

2. Muscle excitability testing with velocity recovery cycles

2.1. Methods

For a convenient introduction to the methods used, the reader is referred to the film at https://www.jove.com/video/60788 and short paper (Witt et al., 2020a,b).

2.1.1. Stimulation and recording

These methods have mostly been applied to *brachioradialis* muscle and *tibialis anterior*, but can also be applied to other muscles. The main requirement is that two or more cm of the muscle are accessible, sufficiently distant from the endplates to avoid stimulating motor axons. In the case of tibialis anterior, this means stimulating and recording at a distance of about 7–8 mm below the surface, since the endplates are located superficially (Aquilonius et al., 1984). We recommend a non-polarisable surface electrode as the anode (e.g. Red Dot, 3 M Health Care, Borken, Germany), and an insulated monopolar needle electrode (25 mm × 26G, TECA, Viasys Healthcare, Madison, Wisconsin, USA) as the stimulating cathode. For BR, the needle electrode is inserted perpendicularly to the muscle at about 25% of the distance from the lateral epicondyle of the humerus to the styloid process of the radius. For tibialis anterior, the stimulating electrode is inserted perpendicularly into the distal third of the muscle, within 1 cm of the palpated distal end (Fig. 1). Stimulation is by rectangular pulses of 50 μs duration, generated by computer and converted to current with an isolated constant current stimulator (e.g. DS7 or DS5, Digitimer Ltd., Welwyn Garden City, Hertfordshire, UK). This technique requires current sufficient to excite a bundle of muscle fibres, causing a small movement of the end of the electrode, but not enough to excite axons and cause a visible twitch of the muscle. Significant axonal stimulation usually results in a marked twitch and discomfort for the subjects, and such recordings are avoided by adjusting the position of the stimulating electrode.

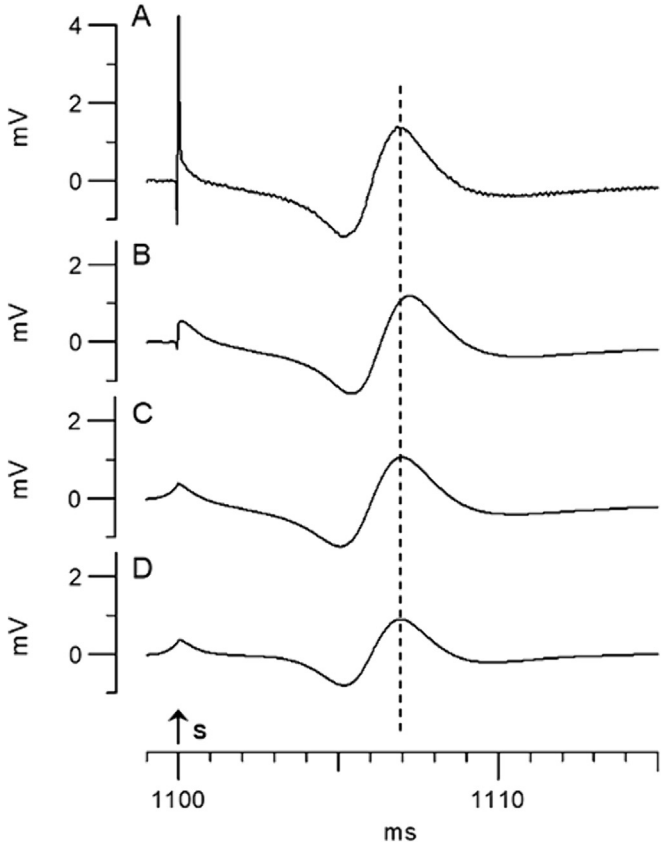

Fig. 3. Fig. 1. Effects of digital filtering on multi-fibre muscle action potentials. (A) Unfiltered trace (bandwidth 1.6 Hz–10 kHz). (B) Effect of single (forward) digital low-pass filter (500 Hz cut-off). (C) Effect of forward–reverse digital lowpass filter (500 Hz) on trace A. The reverse filter cancels out the phase-shifts caused by the forward filter. (D) Effect of combined forward–reverse high-pass (100 Hz) and forward–reverse low-pass (500 Hz) filter on trace A. S indicates time of stimulus. Vertical dashed line marks time of peak of response in D, which was used for the latency measurements. Filtering provides stabilization and smoothing of the baseline without time displacement of the negative peak of the muscle action potential. (N.B. negative action potential peaks are plotted upwards in this and subsequent figures). Reproduced with permission from Boerio et al. (2012b).

For recording, we recommend a disposable concentric needle EMG electrode (25 mm × 30G), inserted perpendicularly approximately 20 mm proximal to the stimulating electrode (Fig. 1). The electrode position is adjusted to obtain a stable triphasic action potential with a minimal stimulus strength (<5 mA). Electrode leads should then be taped to the skin to avoid any electrode movement. A recording gain of 1000, with a bandwidth of about 1.5 Hz–5 kHz, and a sampling rate of 20 kHz is appropriate.

2.1.2. MVRC protocol

Stimulation and recording of muscle velocity recovery cycles have conveniently used QtracW software (copyright UCL Queen Square Institute of Neurology, distributed by Digitimer Ltd, https://www.Digitimer.com) with the recording protocol 1200RCM.QRP, but there is no reason why manufacturers of conventional EMG machines should not program them to make these

recordings, since the stimuli are kept constant throughout. The standard MVRC recordings comprise, in addition to a single conditioning stimulus, stimuli with 2 and 5 conditioning stimuli, separated by intervals of 10 ms. The interstimulus intervals (ISIs), between the last conditioning stimulus and the test stimulus, are decreased in an approximately logarithmic series from 1000 to 1.4 ms, or until conditioned latencies are all greater than unconditioned (see Bostock et al., 2012b for detailed ISI sequence). At each ISI, the stimuli are given in the same sequence, with 0, 1, 2 and 5 conditioning stimuli. With a 2 s interval between each stimulus combination, a full recovery cycle is recorded in less than 5 min (Fig. 2).

2.1.3. MVRC analysis

Here, we describe the analysis method used in the QtracP component of the QtracW software, which is the program used in all the multi-unit MVRC studies published so far. The muscle action potential waveforms, which had been digitized at 20 kHz, were first digitally filtered with high pass and low pass forward-reverse filters, which reduced the bandwidth to 164–320 Hz. This filtering stabilized the baseline and smoothed the waveforms without incurring any time displacement (Fig. 3). The peak of the (inverted) action potential was then interpolated by fitting a quadratic to the top three data points, and then latency was measured from the start of the test stimulus to the interpolated peak, to the nearest 10 μs.

It is clear from Fig. 2 that there is overlap between the responses to the last conditioning stimulus and the test stimulus at short ISIs, and that this is likely to distort the latency measurements. To overcome this, a replica of the response to the conditioning stimulus or stimuli alone was subtracted from the response to the conditioning plus test stimuli (Fig. 4). The replica was obtained by appropriate displacement in time of an earlier trace with longer ISI.

The effects of the conditioning action potentials on the latencies of the test response were calculated as the percentage differences compared to the test stimulus alone (Fig. 5B). The following MVRC parameters, as indicated in Fig. 5B, were routinely measured: MRRP = muscle relative refractory period, the ISI at which a single-conditioned impulse has the same latency as an unconditioned one; ESN, 5ESN = early supernormality, the greatest latency reductions in the first 15 ms following 1 or 5 conditioning stimuli; LSN = late supernormality, the mean latency reduction between 50 and 150 ms following a single conditioning stimulus; 2XLSN, 5XLSN = extra late supernormality following 2 or 5 conditioning stimuli; RSN, 5RSN = residual supernormality, the mean latency reduction between 900 and 1000 ms following 1 or 5 conditioning stimuli. Amplitudes of the test responses, which declined progressively at short ISIs (Fig. 5A) were less consistent between subjects and have not been measured routinely.

2.1.4. Strength of conditioning and test stimuli

The multi-fibre MVRCs described here differ from most recovery cycles in that the conditioning and test stimuli are neither minimal, to excite just a single muscle fibre (as used by (Mihelin et al., 1991), nor supramaximal, to excite all the fibres, as used for nerve excitability cycles (Kiernan et al., 2020; Tankisi et al., 2022). Instead, an intermediate strength of stimulus is used, and the same strength is used for both conditioning and test stimuli. This might be expected to result in very variable recovery cycles, but it turns out that this is not the case. Latencies of multi-fibre muscle action potentials are rather insensitive to stimulus strength over a wide stimulus range (Fig. 6A–C) and MVRCs are insensitive to changes in conditioning stimulus strength over the range 90–150% of the test stimulus (Fig. 6D,E). These findings help to justify the simplicity of using equal submaximal conditioning and test stimuli for the recording of MVRCs.

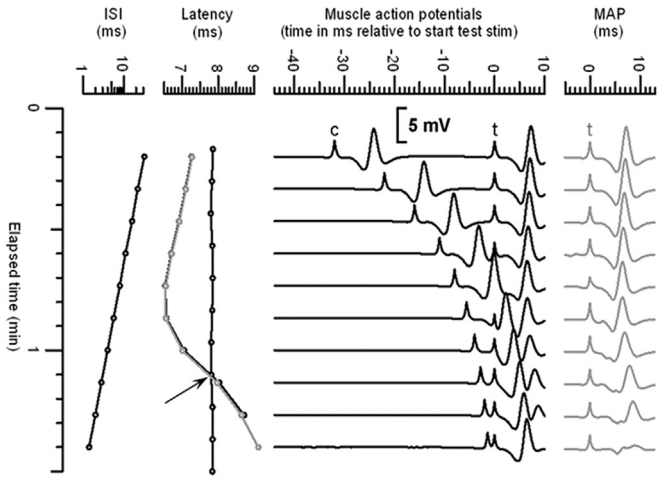

Fig. 4. Method of measuring response latencies when responses to conditioning and test stimuli overlapped. In the centre are plotted in black the muscle action potential responses to conditioning and test stimuli, with c and t indicating respective stimulus artifacts. On the right in grey are plotted the same muscle action potential (MAP) responses after subtraction of a replica of the response to the conditioning stimulus alone. (To the left the ISIs, reducing from 32 to 1.4 ms, are plotted on a log scale, and the measured latencies to peak of the responses to unconditioned and conditioned test stimuli. Grey lines and points indicate measurements made after replica subtraction. Arrow indicates estimate of MRRP from ISI at which lines connecting conditioned and unconditioned test latencies cross. The replica subtraction reduced the MRRP estimate from 3.04 to 2.96 ms. Reproduced with permission from Boerio et al. (2012b).

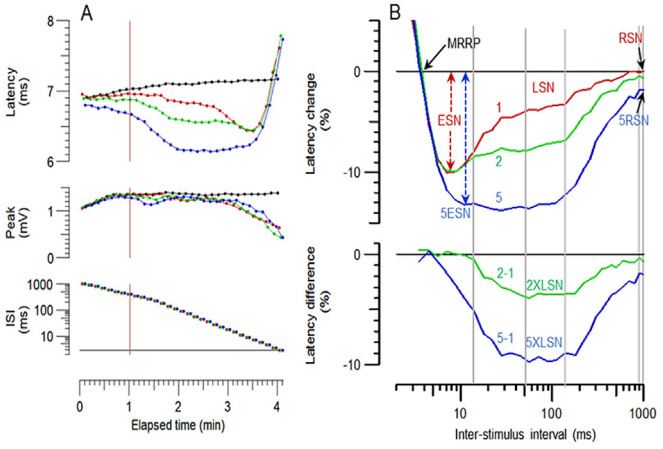

Fig. 5. MVRC measurements. **A**: Latencies and peaks of responses to test stimuli in a healthy control subject after digital filtering and remeasuring. **B**: *Upper plot*: Latencies of conditioned responses in A, replotted as percentage changes from test-alone responses. *Lower plot*: Differences in latency changes from single conditioning stimulus following 2 and 5 conditioning stimuli. Arrows and letters indicate MVRC parameters measured (see text).

2.1.5. Frequency ramp and repetitive stimulation protocols

To explore the effect of more extensive stimulus trains on muscle excitability, a frequency ramp protocol was added (Boerio et al., 2012b). In this protocol, a test stimulus was given every 2 s, as for MVRCs, and from 1 to 30 conditioning stimuli added, spread out at equal intervals over the preceding second (Fig. 7). Further repetitive stimulation protocols have been added to investigate fatigue, using intermittent stimulation at 20 Hz (Boerio et al., 2012a; Tan

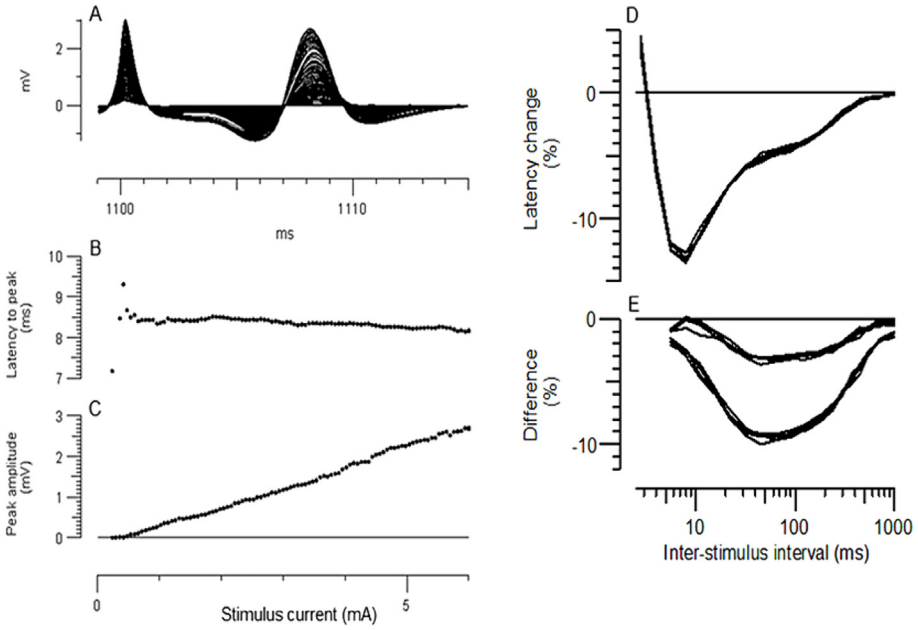

Fig. 6. Effects of varying stimulus strength. Left: Stimulus-response relationship for direct muscle excitation in a healthy subject. A: Superimposed multi-fiber action potentials for stimulus intensities from 0 to 6 mA in 1% steps. B: Latencies to peak of above action potentials. C: Peak amplitudes of muscle action potentials. Latencies varied little with stimulus intensity, whereas peak amplitudes were almost linearly related to stimulus strength, with no sign of saturation. Right: D: Superimposed MVRCs to single conditioning stimuli with strengths of 90%, 100%, 110%, 120% and 150% of test stimulus. E: Superimposed difference plots of 2–1 and 5–1 conditioning stimuli with same 5 stimulus strengths. Reproduced with permission from Boerio et al. (2012b).

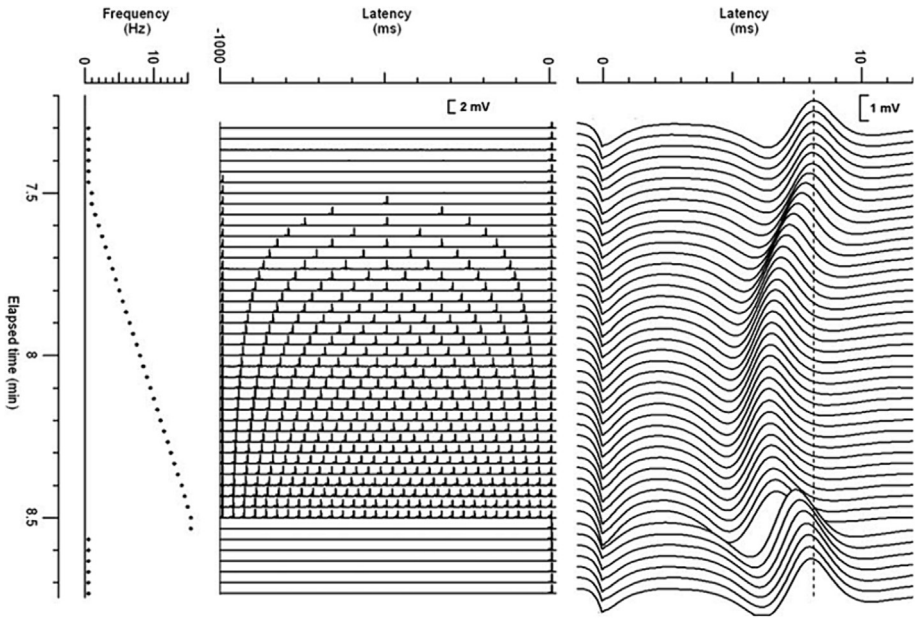

Fig. 7. Example of a frequency ramp recording from *tibialis anterior* in a healthy control subject. Left panel: Mean stimulation frequency. Middle panel: Responses during the period 1 s before and up to 20 ms after the test stimulus. These responses have been half-wave rectified to avoid overlaps. Right panel: Unrectified responses to test stimuli on expanded scale. Vertical dashed line indicates baseline latency to peak of response. Reproduced with permission from Boerio et al. (2012b).

et al., 2020; Tan et al., 2018) and 36.67 Hz (Hochstrasser et al., 2021).

Analysis of frequency ramp data proceeded as for MVRC data, except that measurements were made of the changes in peak amplitude as well as latency, and for the first response in each train as well as the last response. Fig. 8 illustrates the frequency ramp recording from a patient with myotonia congenita, and the points on the recordings where measurements were made.

2.1.6. Practical methodological aspects

2.1.6.1. The duration of the recordings and the success rate. The recording takes approximately 15 min when MVRC and RAMP protocols are combined including the time for preparation. The repetitive stimulation protocol takes approximately 30–40 min.

It is rare that one should completely fail to obtain a recording; however, this may occur in end-stage disease where the muscle fibres have been largely replaced by connective tissue or fat. In

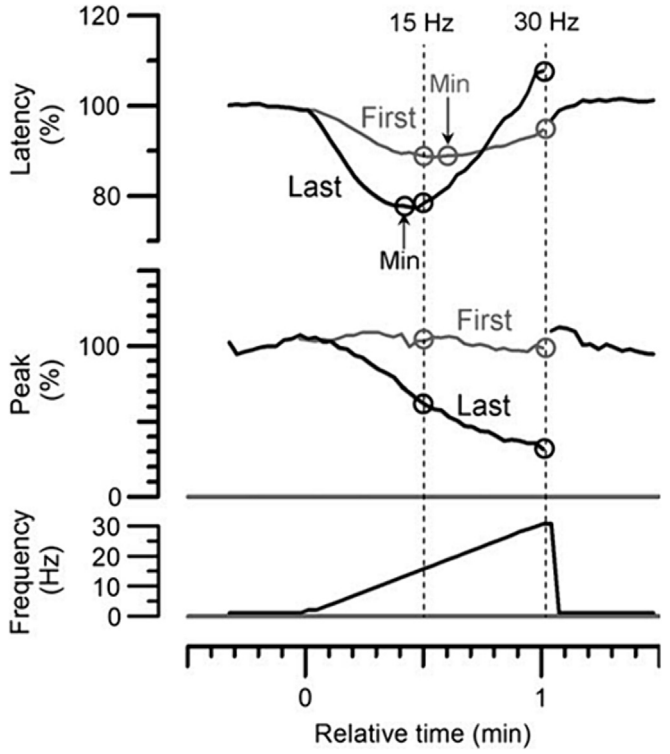

Fig. 8. Frequency ramp measurements. Changes in latency and peak of muscle action potentials in a patient with myotonia congenita during the frequency ramp protocol, in which a 1-s train of impulses was given every 2 s. During the period of the frequency ramp, separate measurements were made of the responses to the first and last stimulus in the train. Small circles indicate points measured when intermittent stimulation was at 15 or 30 HZ, and also the frequencies when latency was minimal; for example, Lat(15HZ)First(%) = % change in latency of first response in train, when frequency reached 15 HZ, FLatMinLast(HZ) = frequency when the latency to the last response in the train was minimal. Reproduced with permission from Tan et al. (2014).

healthy muscle, recordings are generally successful in all individuals. Even with moderate-severe muscle pathology, although it may be slightly more difficult, it is usually possible to obtain a successful recording. However, the success rate may differ if the examiner is not trained.

2.1.6.2. Tolerability. The examination is generally very well-tolerated. Since the stimulus intensity must be less than 10 mA, and in most cases, a stimulus intensity of around 5 mA is used, the subjects rarely complain about discomfort.

2.1.6.3. Indications for protocol selection and interpretation. We recommend that the MVRC and frequency ramp protocols be performed on each subject, since the parameters ESN, MRRP and the ramp latency changes (e.g. at 15 Hz) are very sensitive indicators of muscle membrane depolarization. In the case of suspected channelopathies, other parameters become more important, as described in Section 5.

Additionally, it is a virtue of the muscle excitability measures, like nerve excitability ones like threshold electrotonus, that they provide qualitative information about membrane abnormalities, and not just an indication of membrane potential. However, this extra information inevitably comes at the expense of additional complexity, making interpretation more difficult.

3. Normal findings and studies in healthy subjects

Table 1 summarizes the studies using MVRC recordings that have been done in healthy subjects. The technique of recording MVRCs was originally developed for brachioradialis, due to its well-defined and small endplate zone (Z'Graggen and Bostock, 2009). Test-retest reliability for brachioradialis recordings repeated after a week by the same operator was found to be 'excellent' for ESN (ICC = 0.90), and 'fair to good' for MRRP (ICC = 0.51) (Z'Graggen et al., 2011a). Coefficients of repeatability, indicating how large a change has to be to be considered significant, were 2.6% for ESN and 0.85 for RRP, i.e. about 25% of prior value in each case (Z'Graggen et al., 2011b). Later, the technique was also used for recordings from tibialis anterior (Boerio et al., 2012b). The MVRC recordings from tibialis anterior did not differ significantly from recordings in the same subject made from brachioradialis by the same examiner (Wilcoxon paired comparison *P* values for all MVRC parameters > 0.11). Furthermore, MVRC recordings from tibialis anterior performed in two different cohorts of healthy subjects at two different laboratories by two different examiners were very similar (Mann-Whitney unpaired comparison *P* values all >0.58) (Boerio et al., 2012b). In contrast, MVRC recordings from the rectus femoris muscle show distinct variations compared to recordings from tibialis anterior with a shift of the MVRC curve to the right and upwards (prolongation of MRRP, reduction of ESN and LSN) (Lee et al., 2019b), which might reflect the anatomical muscle position and its anti-gravity function. In general, recordings from the tibialis anterior muscle are easier to perform due to the geometric conditions and the muscle characteristics, resulting in a lower probability of displacement of the stimulating and recording needles. In healthy subjects, it has been shown that MVRC recordings can also be performed using surface electrodes for recording instead of a concentric EMG needle (Z'Graggen et al., 2016a). While recordings with surface electrodes are facilitated by the fact that the precise positioning of the recording needle is no longer required, the stimulus responses have significantly smaller amplitudes, which in the case of muscle pathologies may mean that MVRCs can no longer be recorded. This may be the reason why surface recordings have not been used in patients with myopathies so far.

MVRC recordings have been shown to be highly sensitive to temperature (Bostock et al., 2012a) and show a slight dependence on serum electrolytes: MRRP is dependent on potassium and LSN on bicarbonate (Boland-Freitas et al., 2022). One study focused on the variability and repeatability of MVRC recordings and showed good reliability of the technique, which therefore allows comparison of muscle membrane function both within subjects over time and between groups (Z'Graggen et al., 2011b). In this study, no association was found between age and muscle excitability, however, the results of a later study that included a sample with a wider age range, suggest that progressive depolarization of the muscle membrane occurs with normal ageing (Lee et al., 2018).

Four further studies in healthy volunteers aimed to manipulate muscle membrane function and capture this using MVRC recordings. During experimental ischaemia of the examined muscle, the affected muscle fibre membranes increasingly depolarized as shown by a prolonged MRRP and reduced ESN (Z'Graggen & Bostock, 2009) with a high time resolution. Muscle fatigue simulated with 37 Hz muscle fibre stimulation resulted in a decrease of ESN in the beginning of high frequency stimulation, which recovered to baseline before the end of stimulation, while LSN showed progressive changes during stimulation with delayed normalization after the end of high-frequency stimulation (Hochstrasser et al., 2021). Strength training had the opposite effect on muscle fibres: a 14-day strength training leads to hyper-

Table 1
Studies in healthy muscles.

Publication	Aim	Stimulation protocol	Findings	Interpretation
Muscle velocity recovery cycles: effects of repetitive stimulation on two muscles Boerio et al., 2012a,b	MVRC of tibialis anterior and brachioradialis muscles, inter-investigator dependency of recordings	MVRC with 1, 2, and 5 conditioning stimuli; frequency ramp; intermittent 20-Hz stimulation	No differences in MVRC parameters. No investigator dependency	MVRC provide consistent assessment of muscle membrane function
Physiological differences in sarcolemmal excitability between human muscles Lee et al., 2019a,b	Comparison of rectus femoris and tibialis anterior muscles	MVRC with 1 conditioning stimulus	tibialis anterior muscle: MRRP↑, ESN↓, LSN↓ compared to rectus femoris muscle	Results indicate a less negative resting membrane potential in the tibialis anterior muscle, may reflect the effects of muscle function
Muscle velocity recovery cycles: Comparison between surface and needle recordings Z'Graggen et al., 2016	Comparison of MVRC recorded with surface and needle electrodes	MVRC with 1 and 2 conditioning stimuli	Smaller action potentials when recorded with surface electrodes. No difference in MVRC parameters	It is possible to record MVRCs with surface electrodes in healthy subjects
Velocity recovery cycles of human muscle action potentials: repeatability and variability Z'Graggen et al., 2011a,b	Variability and repeatability of MVRC	MVRC with 1 and 2 conditioning stimuli	High intraclass correlation of ESN. MVRCs not dependent on electrode spacing, conduction time or velocity. No sex or age dependency	MVRCs allow to compare muscle membrane function both within subjects and between groups
Sarcolemmal excitability changes in normal human aging Lee et al., 2018	Effect of age on MVRC	MVRC with 1, 2, and 5 conditioning stimuli	Increasing age was linearly associated with MRRP↑ and ESN↓	The results suggest a progressive depolarisation of the resting membrane potential with age
Temperature dependency of human muscle velocity recovery cycles Bostock et al., 2012a,b	Temperature dependency of MVRC	MVRC with 1 conditioning stimulus	Cooling: MRRP↑, ESN rather insensitive, LSN not affected	When adequate temperature control is not possible, ESN should be considered
Velocity recovery cycles of human muscle action potentials and their sensitivity to ischemia. Z'Graggen and Bostock, 2009	Effect of ischemia on MVRC	MVRC with 1 and 2 conditioning stimuli	Ischemia: MRRP↑, ESN↓	MRRP and ESN are sensitive to muscle membrane potential
Serum electrolyte concentrations and skeletal muscle excitability *in vivo* Boland-Freitas et al., 2022	Effects of serum electrolytes on MVRC	MVRC with 1, 2, and 5 conditioning stimuli; frequency ramp	Repeated MRRP and frequency ramp correlate positively with potassium, LSN negatively with bicarbonate	Potassium and bicarbonate may be of importance for the interpretation of MVRC
Effect of Intermittent High Frequency Stimulation on Muscle Velocity Recovery Cycle Recordings Hochstrasser et al., 2021	Effect of intermittent high-frequency stimulation on MVRC	MVRC with 1 and 2 conditioning stimuli; intermittent 37-Hz stimulation	Initial ESN↓, recovering during stimulation; LSN↓	MVRC can depict changes of membrane potential during exercise
Force training induces changes in human muscle membrane properties Z'Graggen et al., 2016	Effect of force training on MVRC	MVRC with 1, 2 and 5 conditioning stimuli	MRRP↓, ESN↑, LSN unchanged	MVRC show training induced hyperpolarisation of resting membrane potential
Exploring the peripheral mechanisms of lower limb immobilisation on muscle function using novel electrophysiological methods Zeppelin et al., 2023	Effect of short-term immobilisation and subsequent retraining on MVRC	MVRC with 1, 2, and 5 conditioning stimuli; frequency ramp	Immobilisation led to a MVRC parameters not affected, except for a slight MRRP↑	MVRC are not affected by immobilisation and training

ESN, early supernormality; LSN, late supernormality; MRRP, muscle relative refractory period; MVRC, muscle velocity recovery cycle.

polarization of the trained muscle fibres (Z'Graggen et al., 2016). A short-term immobilization period of the respective muscle had no effect on muscle excitability (Zeppelin et al., 2023).

4. Myopathies

4.1. Uraemic myopathy

Uraemic myopathy is seen in end-stage renal disease and is characterized by functional and occasionally structural muscle abnormalities (Campistol, 2002). The cause of uraemic myopathy is proposed to be the uraemic state itself, and hyperkalaemia and acidosis are suggested to be the pathophysiology behind the functional abnormalities without structural changes in muscle fibres (Sinha & Agarwal, 2013; Z'Graggen et al., 2010).

MVRC examinations have the unique possibility to show immediate changes in muscle membrane properties such as intervention studies and the effect of hemodialysis. End-stage renal disease was one of the first disorders MVRC was applied, and this study showed depolarization of the muscle membrane mainly caused by hyperkalemia (Z'Graggen et al., 2010). In a recent study, the depolarisation of the muscle membrane was verified in 18 patients with end-stage renal disease (Larsen et al., 2021). This study could further elucidate the pathophysiology of uraemic myopathy by including an additional 5 conditioning stimuli to the MVRC protocol and a frequency ramp protocol to detect the changes to repetitive stimulation. MVRC and frequency ramp parameters showed depolarization before and normalization at the end of haemodialysis, and these changes were correlated to serum potassium levels suggesting that the muscle membrane depolarisation is mainly due to hyperkalaemia. The results of this study suggested that potassium-induced depolarization may also be the mechanism behind muscle fatigue and weakness in end-stage renal disease (Larsen et al., 2021). In this study, quantitative electromyography (qEMG) showed myopathic changes only in one of the 18 patients.

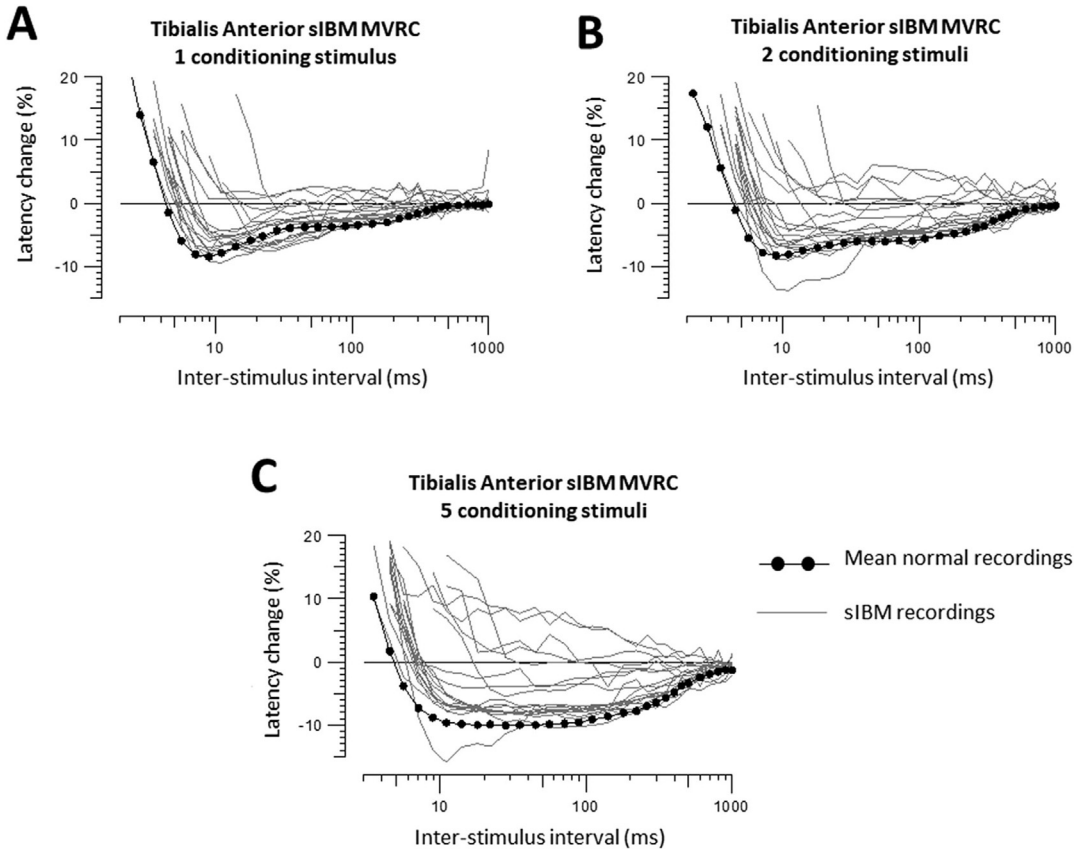

Fig. 9. MVRC latency changes in sporadic inclusion body myositis (sIBM) patients versus controls. A. MVRC recordings with 1x conditioning stimulus. B. MVRC recordings with 2x conditioning stimuli. C. MVRC recordings with 5x conditioning stimuli. Grey curves represent individual sIBM patients and the black circles indicates the mean of normal controls. Reproduced with permission from Lee et al. (2019a).

4.2. Critical illness myopathy

Critical illness myopathy (CIM) is a frequent cause of muscle weakness and weaning failure in critically ill patients (Z'Graggen & Tankisi, 2020). The diagnosis of CIM is possible with nerve conduction studies, electromyography, and muscle biopsy, however, these methodologies detect advanced changes which are first evident after weeks. Therefore, methodologies for the detection of early changes are needed.

The first application of MVRC in 10 probable CIM patients showed abnormal excitability properties, i.e. prolonged MRRP and decreased ESN indicating muscle membrane depolarization and/or increased sodium channel inactivation (Z'Graggen et al., 2011a). We propose the inactivation of the sodium channel ($Na_V1.4$) for the possible mechanisms for CIM based on earlier reports (Haeseler et al., 2008) showing that lipopolysaccharides interact with voltage-gated sodium channels, reducing channel availability at depolarized membrane potentials. In a later study, MVRC was applied in 24 patients with ICU-acquired weakness, i.e. critically ill patients with muscle weakness and/or weaning failure. In this study, an additional 5 conditioning stimuli to MVRC and a frequency ramp protocol were applied. MVRC and frequency ramp parameters showed muscle membrane property changes with up to 100% sensitivity and specificity whereas myopathic qEMG was seen in 63% of the patients (Tankisi et al., 2021).

In a recent study, longitudinal MVRC and frequency ramp recordings were performed in critically ill adult COVID-19 patients requiring mechanical ventilation on Days 1, 2, 5, and 10. CIM diagnosis was made based on clinical, electrophysiological, and muscle biopsy data, and of the 31 patients, 17 developed CIM and 14 patients did not. On Day 10, MVRC and frequency ramp parameters could discriminate between the two groups with a diagnostic precision of 90% (AUC 0.908; sensitivity 1.000; specificity 0.714), on Day 1 with a diagnostic precision of 73% (AUC 0.734; sensitivity 0.562; specificity 0.857) and on Day 2, 82% (AUC 0.820; sensitivity 0.750; specificity 0.923). This study suggests that muscle excitability testing may be a promising method for early diagnosis of CIM and monitoring whether CIM will develop or not (Rodriguez et al., 2022).

Animal studies in a pig sepsis model (Boerio et al., 2018) and in a porcine faecal peritonitis (Ackermann et al., 2014) showed similar changes as human CIM MVRC and frequency ramp recordings.

4.3. Inclusion body myopathy

Sporadic inclusion body myopathy (sIBM) is one of the commonest acquired myopathies in the elderly. Various hypotheses exist as to the pathophysiology of this disease with proponents for inflammatory and degenerative mechanisms as the original process (Needham & Mastaglia, 2016). The most common muscles affected are the long finger flexors and quadriceps complex, and slow progression is assured. Infrequently, bulbar muscles are affected, meaning morbidity rather than mortality is more important (Benveniste et al., 2011). In a muscle excitability study of 20 patients vs 22 similar age matched controls using both tibialis anterior and rectus femoris muscles (Fig. 9), high MRRP and low ESN were noted in patients (Lee et al., 2019a). These measures imply a state of sarcolemmal depolarization which was not confounded by electrolyte or temperature differences given the sim-

ilarities in these parameters between the two groups. These findings led the authors to conclude this may be supportive evidence for previous observations that amyloid beta (Aβ) protein can disrupt Na^+K^+ pump function either directly (Mukhamedyarov et al., 2014) or via an effect on mitochondria (Boncompagni et al., 2012). An alternative explanation is preferential loss of Type II fibres in sIBM. However, neither of these parameters correlated with clinical scores of severity such as disease duration, measures of functionality or quadriceps muscle strength. Late supernormality (LSN), a parameter related to t-tubule function, appeared decreased in tibialis anterior but not rectus femoris, when using single or multiple conditioning stimuli. Only LSN to multiple conditioning stimuli in rectus femoris, correlated to quadriceps strength. This may relate to inflammatory processes affecting the t-tubular network, but independence of this variable from ESN changes cannot be assured. Reduced latency reduction in the ramp protocol was felt to be secondary to membrane depolarisation.

4.4. Other myopathies

Muscle excitability testing showed in a group of patients with hereditary and acquired myopathies the potential of these tests in understanding disease pathophysiology in myopathies (Meldgaard et al., 2023). The MVRC and frequency ramp parameters could discriminate between healthy controls and myopathy patients, more significantly for non-inflammatory myopathy. MVRC differences with normal MRRP in non-inflammatory (hereditary) myopathy differed from other conditions with membrane depolarisation. This study suggested that the pathogenesis in non-inflammatory myopathy does not seem to be caused by a depolarisation of the resting membrane potential but one could hypothesize the change in sodium channels of the muscle membrane as a possible mechanism (Meldgaard et al., 2023).

5. Muscle ion channelopathies

The muscle ion channelopathies comprise a spectrum of clinical disorders arising from mutations in muscle ion channel genes that result in alterations in the excitability of skeletal muscle. Ion channel function can also be affected by mutations in non-ion channel genes, as in myotonic dystrophy types 1 and 2 where the unstable tri- and tetranucleotide repeats respectively, lead secondarily to impaired function of the muscle chloride ion channel. Increased muscle excitability typically manifests as myotonia or muscle spasms, and reduced muscle excitability as weakness or paralysis. However, these clinical features characteristically show marked variability in intensity and duration, especially in the early stages, and may be provoked by various combinations of exercise, rest, diet and changes in serum electrolyte levels. Since the mechanisms underlying these unusual manifestations appear to involve the interplay of many different physiological processes, muscle excitability studies, which measure (indirectly) real time changes in muscle membrane potential using a variety of stimulation protocols (mimicking different types of muscle activation) offers a unique opportunity to study the physiological consequences of a mutation on ion channel function *in vivo*, and have proved particularly helpful in providing complementary insights to *in vitro* expression studies. Excitability measures reflect not only changes occurring as a direct consequence of the mutant channel, but also secondary changes resulting from compensatory mechanisms or interactions with other ion channels. Thus, taken together with the expression data, muscle excitability studies enable a clearer understanding of the actual consequences of a specific ion channel mutation to muscle function *in vivo*.

The main changes in the muscle excitability measures for the various muscle ion channelopathies studied (Tan et al., 2020; Tan et al., 2016; Tan et al., 2012; Tan et al., 2014; Tan et al., 2018) are summarised in Tables 2-4, and the interpretation and relevance of the findings are outlined in the text below.

Table 2
Summary of Muscle Excitability findings in the Chloride Channel myotonias & Myotonic Dystrophy types 1 & 2.

Muscle Channelopathy	Ion Channel dysfunction	Muscle Velocity Recovery Cycle	Frequency Ramp
Myotonia Congenita (MC)* (Tan et al 2014)	↓Chloride conductance (CLC-1)	↓Relative Refractory Period; ↑Early Supernormality to 1 & multiple CS; ↑Supernormality at 20 ms; ↑Late Supernormality to 1 and multiple CS; ↑Extra Residual Supernormality to multiple CS, but not to a single CS.	↑Lat reduction at 15 Hz stimulation ↑Rate at which the lat reached nadir and rounded the 'U' ↓Amp of the last in train at 30 Hz
Comparison of ADMC v ARMC	↓Chloride conductance (CLC-1)	No significant differences in MVRC of ADMC and ARMC	Greater fall in amp in ARMC at 15 Hz and above (No significant amp change in ADMC v NC)
MC TREATED WITH Na channel blockers v MC on NO TREATMENT	↓Chloride conductance (CLC-1) + therapeutic ↓Na^+ conductance	Reduced and delayed onset of Early Supernormality to multiple CS; mild reduction in Late Supernormality to multiple CS	
Effect of Mexiletine in Healthy volunteers (Ruijs et al 2022)	↓ Na^+ conductance	Reduced Early Supernormality and Extra Late Supernormality to multiple CS	Lat reduced by less & reached minimum at lower stimulation frequencies
Myotonic Dystrophy type 1 (DM1) (Tan et al 2016; Boland-Freitas et al., 2018)	↓*DMPK* ↓ Na^+ current (silencing of Na^+ channels) ↓Na^+/K^+ pump activation *RNA toxicity* ↓Chloride conductance	↓Supernormality at 20 ms to multiple CS (weak DM1 patients only, Tan et al 2016) ↑Relative Refractory Period, ↓Early Supernormality in advanced DM1 (Boland-Freitas et al., 2018) ↑Extra Residual Supernormality to multiple CS (all DM1)	↓Lat 30 s after end of frequency ramp (weak DM1 patients only), no abnormalities in strong DM1 patients (Tan et al 2016). ↓Amp at high frequency in advanced DM1 (Boland-Freitas et al., 2018)
Myotonic Dystrophy type 2 (DM2) (Tan et al 2016; Boland-Freitas et al., 2018)	↓*CNBP & RNA toxicity* ↓Chloride conductance	↑Extra Residual Supernormality to multiple CS	No abnormalities

CS: conditioning stimuli; Lat: latency; Amp: amplitude.
* Comparison of Dominant (ADMC) & Recessive (ARMC) patients NOT ON TREATMENT with sodium channel blockers v Normal Controls.

Table 3
Summary of Muscle Excitability findings in the Sodium Channel myotonias.

Muscle Channelopathy	Ion Channel dysfunction	Clinical manifestation	Muscle Velocity Recovery Cycle	Frequency Ramp	Repetitive Stimulation
Sodium channel myotonia (Tan et al 2018)	↑inward Na^+ current ($Na_v1.4$) (e.g. ↓fast inactivation &/or ↑activation)	Myotonia	↓ Relative Refractory period ↑Early Supernormality to 1 and multiple CS; ↑Supernormality at 20 ms to multiple CS; ↑Late Supernormality to multiple CS; ↑Residual Supernormality	↑Lat reduction at 15 Hz stimulation	↓Relative Refractory Period at baseline & throughout 20 Hz stimulation cycles ↑Early Supernormality & ↑Late Supernormality at baseline, and throughout the 20 Hz stimulation cycles (without reduction in supernormality seen in NC during Rep Stim)
Paramyotonia Congenita	↑inward Na^+ current ($Na_v1.4$) with non-inactivating persistent Na^+ currents*	Myotonia (paradoxical) + exercise/cold-induced weakness	↑Early Supernormality to multiple CS; ↑Supernormality to one and multiple CS at 20 ms; ↑Late Supernormality to multiple CS; ↑Residual Supernormality to multiple CS	↓Amp during Ramp with frequencies > 10 Hz, unrecordable at high frequencies, partial recovery 30 s after end of frequency ramp; ↑Lat at of first in train at 30 Hz stimulation	↑Relative Refractory period at baseline (unmeasurable during Rep Stim) ↓Amp at start of Rep Stim; no recovery post-20 Hz stimulation for the 10 min recorded.

CS: conditioning stimuli; Lat: latency; Amp: amplitude; Rep Stim: repetitive stimulation; NC: normal controls.
* e.g. ↓fast inactivation &/or ↑activation, faster recovery from inactivation, with cold induced left-shift of activation and disruption of final extent of inactivation

Table 4
Summary of Muscle Excitability findings in the Periodic Paralyses.

Muscle Channelopathy	Ion Channel dysfunction	Clinical manifestation	Muscle Velocity Recovery Cycle	Frequency Ramp	Repetitive Stimulation
Hyperkalaemic Periodic Paralysis (Tan et al 2020)	↑inward Na^+ current ($Na_v1.4$), 'window' currents*	Periodic paralysis +/- myotonia with ↑[K^+]	↑Extra Mean Supernormality to multiple CS; ↑Extra Residual Supernormality to multiple CS	Changes from NC not significant, but in opposite direction to HypoPP	Changes from NC in opposite direction to HypoPP. HyperPP v HypoPP significant for Relative Refractory Period after 20 Hz Rep Stim, and baseline Early Supernormality, Late Supernormality, & Lat. No significant difference HyperPP v NC.
Hypokalaemic Periodic paralysis (HypoPP) types 1&2	Aberrant gating pore current in $Ca_v1.1$ (HypoPP1), $Na_v1.4$ (HypoPP2)	Periodic paralysis with ↓[K^+]	↑Relative Refractory Period ↓Early and Late Supernormality to single and multiple CS	Delay in onset of change in lat, and ↓lat reduction throughout frequency ramp	↑Relative Refractory period at baseline, greater post 20 Hz Rep Stim cycles and persisting above pre-stimulation baseline for subsequent 10 min recorded ↓Baseline Early and Late Supernormality
Andersen-Tawil Syndrome (Tan et al 2012)	↓Kir2.1 conductance	Periodic paralysis/periodic focal weakness, ventricular dysrhythmias, developmental anomalies	↑Relative Refractory Period ↓Extra Late Supernormality to multiple CS		↑Relative Refractory Period at baseline, throughout the 20 Hz stimulation cycles, persisting for the 3 min measured post Rep Stim ↓Early Supernormality post 20 Hz repetitive cycles ↑Lat of the last response in train at 20 Hz

CS: conditioning stimuli; Lat: latency; Amp: amplitude; Rep Stim: repetitive stimulation; NC: normal controls.
* e.g. hyperpolarised shift of activation curve + depolarised shift in midpoint of slow inactivation curve.

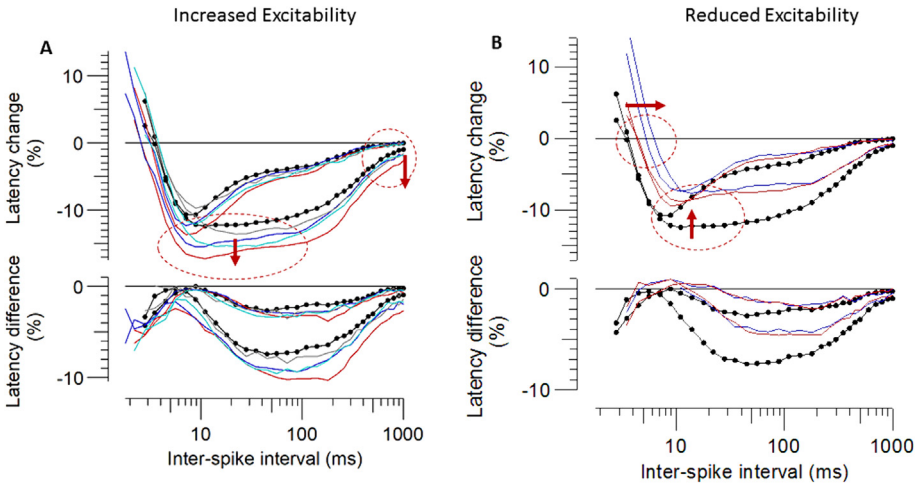

Fig. 10. MVRC latency changes. A. Channelopathies associated with myotonic discharges showing increased early, late and residual supernormality, particularly following multiple conditioning stimuli. NC – black filled circles; MC – red lines; SCM- blue lines; PMC – cyan lines; HyperPP grey lines. B. Channelopathies associated with periodic paralysis without myotonia showing reduced early supernormality and increased muscle relative refractory period. NC – black filled circles; ATS – red lines; HypoPP 1 + 2 – blue lines (data from patients in Tan et al., 2020; Tan et al., 2012; Tan et al., 2014; Tan et al., 2018). (For interpretation of the references to colour in this figure legend, the reader is referred to the web version of this article.)

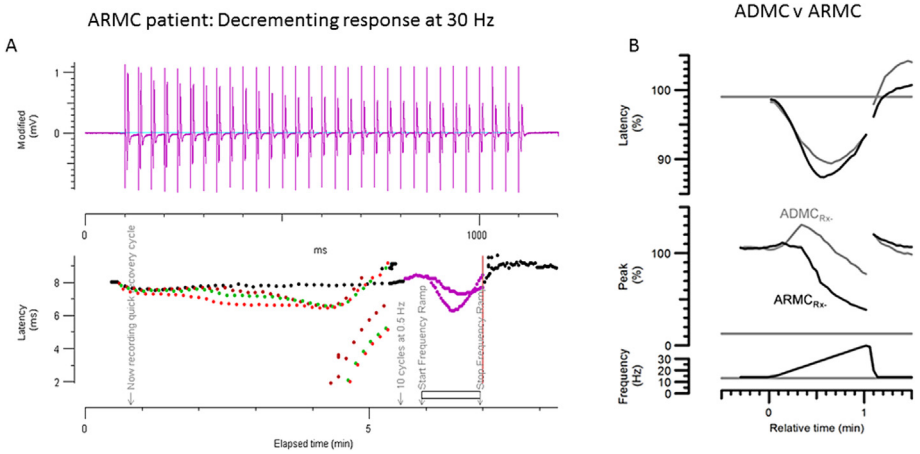

Fig. 11. A. Top panel – Decrementing compound multifibre response to 30 Hz stimulation during the ramp in a patient with ARMC. Bottom panel – latency changes during a recording of MVRC followed by the frequency ramp, with the vertical line marking the time at which the amplitude changes in the top panel are shown. B. Comparison of the latency and amplitude changes during the ramp in five ARMC patients (black) compared with 5 ADMC patients (gray) not on treatment with sodium channel blockers (Tan et al., 2014).

5.1. Patterns of change in the MVRC

Although the types of ion channels and the underlying ion channel dysfunction differ in the various muscle ion channelopathies, there are broad patterns of change in the MVRC profile that are common amongst the disorders associated with increased muscle fibre excitability/clinical myotonia, and those seen in disorders typically associated with reduced muscle fibre excitability/clinical weakness or paralysis.

The MVRC in ion channelopathies associated with myotonic discharges typically show a normal or reduced relative refractory period, with increased early, late, and residual supernormality, the latter often exacerbated by trains of action potentials, and reflecting residual depolarisation on the membrane due to delayed/incomplete repolarisation. This results in a propensity for spontaneous myotonic potentials following muscle activation.

By contrast, in the ion channelopathies associated with weakness or paralysis, the MVRCs (in the interictal state) typically show changes in the opposite direction with increased muscle relative refractory period, reduced early and late supernormality, and no changes in residual supernormality, a pattern consistent with depolarisation of the resting membrane potential (Fig. 10).

5.2. Myotonic disorders

5.2.1. Chloride channel dysfunction

5.2.1.1. Myotonia congenita (recessive and dominant). Myotonia congenita is caused by mutations of the CLCN1 gene, encoding the skeletal muscle chloride channel CLC-1. In general, the recessive form (ARMC) is caused by loss-of-function mutations of both fast gates, whereas in the dominant form (ADMC) there is a depolarised shift in the voltage gating of the common gate. ARMC is typically associated with more severe manifestations, with prominent myotonia and muscle hypertrophy, transient weakness on muscle activation from rest, and a greater decrement in CMAP amplitude on the short exercise test (Fournier et al., 2006; Tan et al., 2011).

The changes in the muscle excitability parameters during the MVRC and frequency ramp protocols are presented in Table 2.

Comparisons are shown between MC patients not on treatment with sodium channel blockers and normal controls; ADMC versus ARMC patients; and MC patients treated with sodium channel blockers (mexiletine, except for one patient on carbamazepine and quinine) versus untreated MC patients (Tan et al., 2014). The effect of mexiletine on healthy volunteers (Ruijs et al., 2022) is presented for comparison.

In keeping with the pattern of MVRC profile seen in myotonic disorders described earlier, untreated MC patients showed an increase in early and late supernormality, and a marked increase in residual supernormality after multiple conditioning stimuli (CS), caused by reduced chloride buffering of the excess potassium in the t-tubules (Table 2). However, contrary to what would be expected with loss of a major component of the resting membrane conductance (based on animal studies which estimated chloride conductance as constituting 80–85% of the resting skeletal muscle membrane conductance), there was no evidence of slowing of the decay of the supernormality after a single conditioning stimulus (Table 2, Fig. 11). If chloride conductance was indeed as high as 80%, the predicted increase in the membrane time constant should have resulted in a clear slowing of decay, but this was not seen, neither for the group as a whole, nor in the ARMC or ADMC patients. The only difference was limited to the brief period up to 100 ms after the action potential (max at 20 ms), suggesting that chloride channels only played a major role in normalizing the membrane potential when the membrane had been depolarised by excess potassium in the t-tubules. Consistent with this, after multiple CS, there was a clear delay in decay of the supernormality. This suggests that chloride conductance in *resting* human muscle is much lower than once thought. These findings are consistent with more recent *in vitro* studies in which internal ATP levels were correctly controlled (DiFranco et al., 2011), and subsequent studies showing a species difference in the resting chloride conductance of human versus rodent skeletal muscle (Pedersen et al., 2009; Riisager et al., 2016). These findings emphasize the advantage of direct *in vivo* study of human muscle physiology.

Differences between the excitability studies of dominant and recessive MC were only significant during the frequency ramp (Table 2), where there was a much greater fall in peak amplitude of the last in train with increasing frequency and train length in ARMC patients (Fig. 11). In ARMC the loss of the buffering effect of chloride conductance leads to the membrane becoming progressively more depolarised as the AP trains became longer and faster, with resulting sodium channel inactivation and a fall in amplitude. In ADMC, the amplitude drop is not significant because, in contrast with the ARMC mutations where there is loss of function of the fast gates, the mutations causing ADMC mainly cause a depolarised shift in the voltage dependence of activation of the common gate. Thus, when the membrane depolarises sufficiently with the trains of APs, the common gate eventually opens, and the depolarisation is self-limiting.

Mexiletine was the main sodium channel blocker used as treatment in these patients. For most MC patients, Mexiletine provides only partial symptomatic relief. Some insights into the likely explanation are provided by the muscle excitability changes induced by Mexiletine in healthy volunteers (Ruijs et al., 2022) and MC patients (Table 2). Mexiletine inhibits sodium channels by causing a hyperpolarised shift in the voltage dependence of fast inactivation and has the effect of reducing total inward Na current during the action potential and increasing the relative refractory period, thus partly reversing the changes in the early part of the MVRC in the MC patients. However, it has almost no effect on the residual supernormality, leaving a persistent predisposition to spontaneous discharges.

Recent studies have shown that an important mechanism by which loss of chloride conductance results in myotonic discharges and transient weakness in ARMC is the activation of slow-inactivating Na channels by the residual depolarisation of the membrane caused by the loss of chloride buffering. This small persistent inward sodium current has the effect of potentiating and perpetuating the residual depolarisation on the membrane after a burst of action potentials, thus facilitating recurrent trains of myotonic discharges. With sustained trains of rapid action potentials, the combination of the loss of chloride conductance and the activation of this slow inactivating sodium current predisposes to plateau potentials that are thought to underlie the transient weakness seen in ARMC (Hawash et al., 2017; Myers et al., 2021).

5.2.1.2. Myotonic dystrophy types 1 & 2. Myotonic dystrophy type 1 (DM1) is caused by an expansion of an unstable trinucleotide $(CTG)_n$ repeat of the DM1 protein kinase (DMPK) gene. DMPK is a serine/threonine kinase and has been shown to modulate skeletal

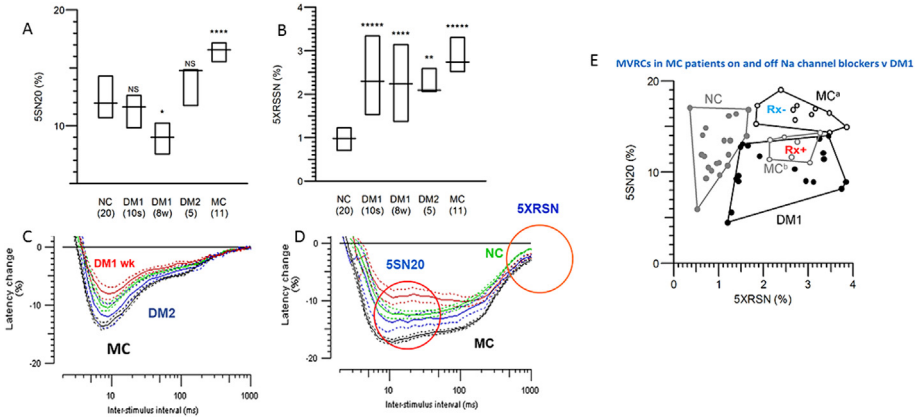

Fig. 12. (A) Latency changes for 5 different groups 20 ms after 5 conditioning impulses, with the DM1 group separated into stronger (10 s) and weaker (8w) subgroups. Boxes indicate interquartile ranges, and lines indicate median values. Comparisons with NC group by Mann–Whitney *U* test indicated as follows: NS 5 $P > 0.05$; *$P < 0.05$; **$P < 0.01$; ***$P < 0.001$; ****$P < 0.0001$; and *****$P < 0.00001$. (B) Similar plots for residual supernormality, 900–1,000 ms after 5 conditioning stimuli. (C) & (D) Reduction in ESN and supernormality at 20 ms to 5 CS in the weak DM1 group (red), compared with NC (green), in contrast to no change in the strong DM1 (light blue), and increased ESN and 5SN20 in the DM2 (dark blue) and MC (black) patients. However, all groups showed increased extra residual supernormality (5XRSN) compared with NC. (E) Effect of sodium-channel blockers on MVRCs in myotonia congenita. Scatterplots of 4 groups, comparing early and late supernormality changes between NC, DM1, and MC patients not on medication (MC^a), and MC patients being treated with sodium-channel blockers (MC^b). (data from Tan et al., 2016). (For interpretation of the references to colour in this figure legend, the reader is referred to the web version of this article.)

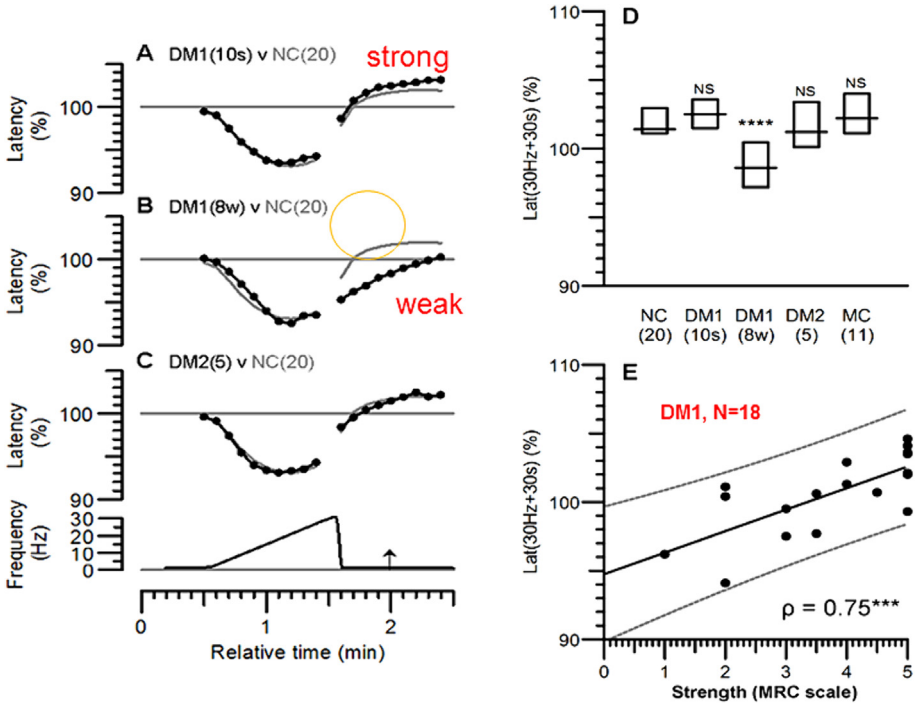

Fig. 13. Effects of the frequency ramp on velocities of muscle action potentials. Left-hand column shows latency changes from baseline stimulation (0.5 Hz) to first stimuli in 1-s trains, which increased from 1 to 30 Hz, and recovery when stimulation reverted to 0.5 Hz. Gray lines: mean of NC group; black circles: mean values for stronger DM1 patients (A), weaker DM1 patients (B), and DM2 patients (C). (D) Latency changes 30 s after end of frequency ramp for 5 groups plotted as in Fig. 1C (****P < 0.0001). (E) Correlation between latency changes 30 s after frequency ramp and muscle strength, according to MRC scale, for 18 DM1 patients (***P < 0.001) (Tan et al., 2016).

muscle sodium channels and calcium homeostasis (Benders et al., 1996; Jacobs et al., 1990). Mechanisms for pathology include RNA toxicity, altered expression of neighbouring genes, and abnormalities in the structure, enzymatic activity, and subcellular localization of the DMPK protein itself. Myotonia is thought to arise due to misregulation of alternative splicing of the muscle chloride channel CLC-1, together with transcriptional downregulation of CLCN1.

Myotonic dystrophy type 2 (DM2), is caused by an unstable tetranucleotide $(CCTG)_n$ repeat expansion in the cellular nucleic acid binding protein (CNBP) gene. As in DM1, the pathogenic effects of the (CCUG)n RNA expansion is thought to underlie much of the features of DM2, although CNBP haploinsufficiency in itself may account for the myotonia, which appears to be due to down-regulation of CLC-1 secondary to low levels of CNPB, without mis-splicing of CLCN1 (Chen et al., 2007).

The muscle excitability findings in DM1 and DM2 (Boland-Freitas et al., 2018; Tan et al., 2016) are summarised in Table 2 and Fig. 12. In common with the MC patients, both DM1 and DM2 patients showed an increase in extra residual supernormality to multiple conditioning stimuli, consistent with reduction in chloride conductance. In the DM2 group, this was the only significant abnormality. Within the DM1 group however, differences were seen in the excitability findings of weak compared with strong DM1 patients (Tan et al., 2016), and in advanced versus less severely affected DM1 patients (Boland-Freitas et al., 2018). In the cohort studied by Tan et al (Tan et al., 2016), the weak DM1 patients showed a reduction in supernormality at 20 ms to multiple conditioning stimuli, without significant change in relative refractory period (Fig. 12), consistent with a reduction in Na^+ channel availability, as observed with DMPK haploinsufficiency in mouse myocytes (Mounsey et al., 1995). Consistent with this, the findings in the weak DM1 patients overlapped with MC patients treated with Na channel blockers (Fig. 12). With more advanced disease (Boland-Freitas et al., 2018) the combination of increased muscle relative refractory period and reduced early supernormality was seen, consistent with depolarization of the resting membrane potential. In the weak DM1 patients (Tan et al., 2016), the frequency ramp revealed a delay in the recovery of the latency to pre-ramp values after cessation of the ramp, and a lack of any post-ramp latency overshoot (Fig. 13). The rapid recovery and overshoot of the latency seen in healthy volunteers is thought to be due to activation and sensitization of the sodium pump to $[Na^+]_i$ by the impulse train. This is thought to be driven by the release of CGRP from sensory nerve endings, which, via cAMP, protein kinase A, and phospholemman, causes an increase in the affinity of Na^+/K^+ ATPase for $[Na^+]_i$ (Buchanan et al., 2002; Shattock, 2009). As phospholemman is a substrate for DMPK, a reduction in DMPK activity in the weak DM1 patients offers a likely explanation for the impaired pump function.

5.2.2. Sodium channel dysfunction

5.2.2.1. Sodium channel myotonia and paramyotonia congenita. Sodium channel myotonia (SCM), formerly known as potassium aggravated myotonia, and paramyotonia congenita (PMC) are both caused by mutations in the transient sodium channel $Na_v1.4$ (SCN4A). Patients with SCM generally have myotonic stiffness which improves with repetition ('warm-up' phenomenon), although in the extraocular muscles, this may sometimes be preceded by transient worsening of myotonia. SCM patients typically do not experience muscle weakness. PMC is characterised by myotonia that paradoxically worsens with repetition (paradoxical myotonia), and experience exercise-related weakness, particularly with muscle exertion at cold temperatures. The weakness may persist after warming and, when severe, may last several hours.

In both SCM and PMC, the mutations are associated with a gain-of-function abnormality of $Na_v1.4$ related to disrupted inactivation or enhanced activation. Slowed fast inactivation lengthens the

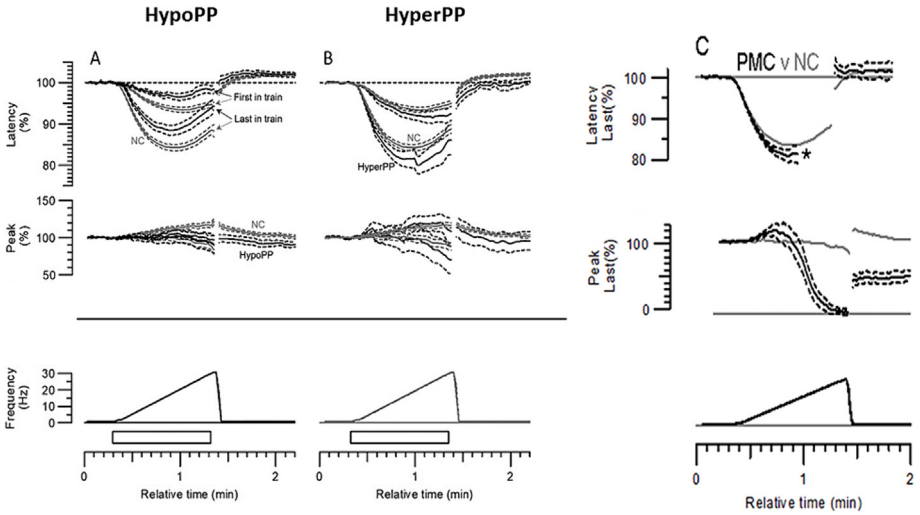

Fig. 14. Frequency ramp in human tibialis anterior muscle. A: Frequency ramp recordings comparing HypoPP patients (black, n = 10) and normal controls (grey, n = 26). B: Frequency ramp for HyperPP patients (black, n = 7) and controls (grey). C: Frequency ramp for PMC (black n = 8) and controls (grey). Lines plotted are means ± standard errors, plotted separately for first impulse in train and last impulse in train, with train frequency increasing linearly to 30 Hz over 1 min. HyperPP: Hyperkalaemic periodic paralysis; HypoPP: Hypokalaemic periodic paralysis; PMC: Paramyotonia congenital (Tan et al., 2020; Tan et al., 2018).

action potential duration, resulting in increased potassium efflux into the t-tubules and a larger after-depolarization which, especially following a train of action potentials, may be sufficiently large to trigger spontaneous myotonic discharges. In some PMC mutations, there is additional disruption of the final extent of inactivation, as well as a cold-induced left shift of the activation curve, causing a more prolonged inward sodium current and more marked depolarisation.

The main muscle excitability changes for SCM and PMC are summarised in Table 3, and the MVRC changes are shown in Fig. 14. In keeping with the presence of clinical myotonia, the MVRC changes were in the direction expected to facilitate repetitive myotonic discharges, with increases in early, late and residual supernormality in both SCM and PMC groups. The larger early supernormality is consistent with a lengthened duration of the muscle action potential due to a slower rate of entry into inactivation in both SCM and PMC, and slowed deactivation in SCM. In the SCM group, despite this, there was a reduction in the relative refractory period, probably due to faster recovery from inactivation described in association with the Val1589Met mutation (Mitrovic et al., 1994), the most common mutation in this study.

Weakness is a feature of PMC, but not of SCM, and the biophysical features of this are demonstrated in the frequency ramp and repetitive stimulation protocols, where, in the PMC patients, there was a rapid decline in the amplitude of the compound multifibre action potential at frequencies above 10 Hz (Fig. 10). The recovery of amplitude to only about 50% of baseline after the ramp, suggests that despite cessation of rapid stimulation, about half the fibres remained in an inexcitable depolarised state, which persisted for the remaining 30 s of the recording, consistent with the clinical observation of post-exercise weakness. All the PMC patients in this study had the Thr1313Met mutation, which has been shown *in vitro* to generate large persistent (non-inactivating) sodium currents (Hayward et al., 1996). Presumably in the fibres that remained depolarised, these currents were sufficiently large as to outweigh the repolarising potassium and chloride currents.

5.3. Periodic paralysis

The familial periodic paralyses are caused by dominant mutations in the skeletal muscle calcium (Ca_v 1.1, CACNA1S), sodium ($Na_v1.4$, SCN4A), or potassium (K_{IR} 2.1, KCNJ2) ion channels. The resultant channel dysfunction destabilises the muscle resting membrane potential such as to predispose it to sustained depolarization, which manifests clinically as episodes of weakness or paralysis.

In hyperkalaemic periodic paralysis (HyperPP), gain-of-function mutations in $Na_v1.4$ predispose to sustained depolarization in high external potassium. In hypokalaemic periodic paralysis (HypoPP), mutations in the S4 voltage sensors of $Ca_v1.1$ (HypoPP1) and $Na_v1.4$ (HypoPP2) result in a gating pore leakage current that makes the membrane susceptible to anomalous depolarization when extracellular potassium is low. In Andersen-Tawil syndrome, mutations affecting the alpha subunit of the inward rectifier potassium channel $K_{IR}2.1$ are associated with variable combinations of periodic paralysis, ventricular dysrhythmias and developmental anomalies. The main excitability changes are summarised in Table 4.

5.3.1. Hyperkalaemic periodic paralysis (Fig. 14)

In keeping with the observation of myotonic discharges in many patients with HyperPP, the MVRC showed an increase in extra mean supernormality and extra residual supernormality to multiple conditioning stimuli. Although early studies using heterologous expression of mutations corresponding to the human HyperPP mutations Thr704Met and Met1592Val in rat sodium channels demonstrated disruption of fast inactivation leading to persistent inward non-inactivating sodium currents similar to those seen in PMC (Cannon & Strittmatter, 1993), in contrast to the PMC cohort, no fall was observed in the amplitude of the compound multifibre response during the frequency ramp or repetitive stimulation in the HyperPP patients. Instead, there were only mild changes (in the opposite direction to that seen in HypoPP) in the relative refractory period and in early and late supernormality, which were not significantly different from normal controls. These findings were much more in keeping with later expression studies of human $Na_v1.4$ channels with the Thr704Met and Met1592Val mutations (Bendahhou et al., 1999; Hayward et al., 1999; Rojas et al., 1999; Yang et al., 1994), which found shifts in the voltage dependence of activation and slow inactivation, with overlaps such as to result in 'window currents'(Bendahhou et al., 2002; Bendahhou et al., 1999; Yang et al., 1994). It is anticipated that with high external

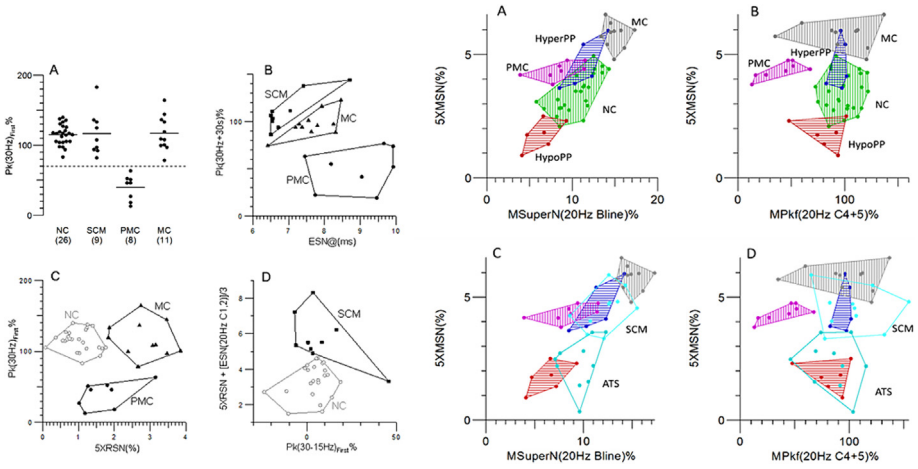

Fig. 15. Separation of groups by combinations of Excitability Measurements. Left panel: Separation of myotonia subtypes. A: The single measurement Pk(30 Hz)First% (i.e. the amplitude of the first action potential in the train at the end of the frequency ramp) separates the paramyotonia congenita patients (PMC) from the normal controls (NC), sodium channel myotonia (SCM) and also the myotonia congenita patients (MC) from a previous study. B: Two measurements, Pk(30 Hz + 30 s)% (i.e. the amplitude 30 s after the end of the frequency ramp) and ESN@(ms) (i.e. the interstimulus interval for peak early supernormality) separate the 3 myotonia subtypes from each other, C: 5XRSN(%) (i.e. the extra residual supernormality at 950–1000 ms following 5 conditioning stimuli) is enhanced in myotonia congenita and with Pk(30 Hz)First% enables separation of NC, MC and PMC. D: sodium channel myotonia patients are separated from normal controls by combining multiple measurements: 5XRSN(%), ESN(20 Hz C1,2) (i.e. the mean early supernormality during the first two cycles of repetitive stimulation oat 20 Hz), and the frequency ramp measurement Pk(30–15 Hz)First% (i.e. the change in amplitude of the response to the first stimulus in the frequency ramp as the frequency is increased from 15 to 30 Hz) (Tan et al., 2018). Right panel: Separation of groups by combinations of MVRC and repetitive stimulation measurements. A: Showing increased extra mean supernormality to 5 conditioning stimuli compared with NC (n = 24) in the conditions associated with myotonia, with a slight differential increase in the baseline supernormality before the start of the 20 Hz trains partially separating the PMC (n = 8), HyperPP (n = 5), and myotonia congenita (MC) (n = 10, MC patients not on sodium channel blockers) groups. The changes are in the opposite direction from NC for HypoPP (n = 6). B: The groups can also be partially separated plotting extra mean supernormality to 5 conditioning stimuli against changes in the amplitude of the first in train for the fourth and fifth cycles during 20 Hz repetitive stimulation. C: As in A, but with NC removed and SCM (n = 10) and ATS (n = 10) data included to show the overlap between SCM and HyperPP, and between ATS and HypoPP. D: as in B, but with NC removed and again showing the overlap between SCM, HyperPP, and MC, and between ATS and HypoPP. (MC data from Tan et al., 2014. ATS data from Tan et al., 2012). ATS: Andersen-Tawil Syndrome; HyperPP: Hyperkalaemic periodic paralysis; HypoPP: Hypokalaemic periodic paralysis; MC: Myotonia Congenita; MVRC: muscle velocity recovery cycle; NC: normal controls; PMC: paramyotonia congenita; SCM: sodium channel myotonia (Tan et al., 2020).

potassium the change in E_K may become sufficient to shift the resting membrane potential into the 'window current' range, resulting in an inactivating inward sodium current that would depolarise the membrane, thereby precipitating a paralytic attack.

5.3.2. Hypokalaemic periodic paralysis types 1 and 2 (Fig. 14)

The muscle excitability findings were similar for both HypoPP1 and HypoPP2 and are summarised together in Table 4. The MVRC showed an increased relative refractory period and reduced early supernormality consistent with depolarisation of the resting membrane potential. In the repetitive stimulation protocol, the delayed and less effective 'correction' of the relative refractory period during trains of action potentials suggests that in the presence of the gating pore current, the Na^+/K^+ pump has difficulty restoring baseline membrane potential after a period of exercise.

5.3.3. Andersen-Tawil Syndrome

In Andersen-Tawil Syndrome, the excitability changes suggest that loss of the potassium inward rectifier $K_{IR}2.1$ conductance results in mild depolarisation, due to less efficient clamping of the resting membrane potential to the equilibrium potential of potassium. Exacerbation of the membrane potential changes with exercise is suggested by the abnormalities in the relative refractory period and early supernormality becoming more marked after the end of the 20 Hz repetitive stimulation cycles.

5.4. Comparisons of excitability properties of the different muscle ion channelopathies

In keeping with there being a general pattern of change in the MVRC for conditions associated with increased and decreased muscle excitability, combinations of excitability measures from all three stimulation protocols revealed a clustering of excitability measures within each ion channelopathy, which generally diverged from normal controls in the same direction amongst the conditions associated with myotonic discharges, and in the opposite direction for those associated with periodic paralysis (Fig. 15). Although the considerable overlap in the polygons in Fig. 15 suggests that excitability measures in isolation are insufficient for a precise identification of the underlying ion channel involved, muscle excitability data can prove particularly helpful in providing complementary data in situations where there is difficulty resolving clinical, genetic and expression study data (Thor et al., 2019).

Overall, the insights gained from muscle excitability studies in these groups of patients have highlighted the fact that despite progress in genetic analysis, there remain clear advantages in having a minimally invasive, reproducible method that allows direct *in vivo* assessment of *human* muscle.

5.5. Axonal neuropathies, ALS, and other clinical conditions

Muscle excitability testing provides an indirect measure of the changes in muscle membrane properties including depolarization and physiological consequences of ion channel dysfunction *in vivo*. However, these measurements are limited to a small area around the tip of the needle electrodes. In a study on ALS patients, MVRCs did not show any abnormality although MScanFit motor unit number estimation (MUNE)values were reduced, there was denervation activity in the same examined muscle and quantitative EMG showed chronic neurogenic changes (Kristensen et al., 2019). In another study on diabetic polyneuropathy, MVRCs were normal despite confirmed polyneuropathy with nerve conduction studies and reduced MScanFit MUNE values (Kristensen et al., 2020).

We propose that we might have sampled healthy muscle fibres while we were adjusting the stimulation and recording needle electrodes. Like nerve excitability testing, muscle excitability tests are most useful for diffuse disorders affecting the whole muscle such as channelopathies, uraemia and myopathy. However, these findings in ALS may reflect the patchy disease pattern of ALS because depolarization has been shown in neurogenic muscles in other conditions including entrapment neuropathies, radiculopathy and spinal cord injury (Witt et al., 2020a, Witt et al., 2020b; Witt et al., 2019). Pronounced changes in MVRC and frequency ramp have also been shown in critical illness myopathy (Tankisi et al., 2021; Z'Graggen et al., 2011a), uraemic myopathy (Larsen et al., 2021; Z'Graggen et al., 2010) and in a cohort of subjects with myopathy of various aetiologies (Meldgaard et al., 2023). For critical illness polyneuropathy, nerve excitability testing seems to be more appropriate (Z'Graggen et al., 2006). Another condition characterized with diffuse alterations on muscle membrane is ischemia (Z'Graggen & Bostock, 2009). Muscle ischaemia induced by a cuff or orthostatic hypotension (Humm et al., 2011) showed muscle membrane depolarisation. Similarly, in a study on leg pain in neuropathic postural tachycardia syndrome was found to be associated with altered muscle membrane properties (Rodriguez et al., 2021).

Showing alterations of muscle membrane properties in real time, following an intervention demonstrates the potency of muscle membrane excitability testing. Therefore, these tests may be potential biomarkers for drug trials. In a recent randomized, double-blind, two-way crossover study, the effects of mexiletine, a voltage-gated sodium channel blocker could be shown in 15 healthy subjects after a single dose of 333 mg mexiletine versus placebo (Ruijs et al., 2022).

6. Animal studies

Not long after the establishment of MVRC recordings in the clinical setting, the technique was also used in animal experiments. In a porcine model of experimental sepsis, MVRC recordings were successfully applied to the study of the early changes in muscle membrane potential preceding the development of critical illness myopathy (Ackermann et al., 2014; Boerio et al., 2018). In pigs, the MVRC recordings could be performed with exactly the same technique as in humans. While MVRC parameters showed slightly different normal values, the MVRC profile was comparable to the ones in humans.

More recently, adaptation of muscle excitability studies to allow in-vivo and ex-vivo MVRC studies of rodent skeletal muscle (Suetterlin et al., 2022; Suetterlin et al., 2021) has enabled the direct study of the effects of various ion channel modulators in rodents. The MVRC studies in mice and rats revealed a 'rodent MVRC profile', which was distinct from the MVRCs of humans and other larger mammals such as pigs (Ackermann et al., 2014; Boerio et al., 2018; Suetterlin et al., 2022; Suetterlin et al., 2021). This probably reflects the physiological adaptations needed for the rapid muscle contractions required to achieve the limb speeds of these small mammals (Suetterlin et al., 2022). Since mouse models remain important for studying disease mechanisms and for exploring possible therapeutic interventions for human disease, the clear differences between rodent and human MVRCs illustrates the importance of understanding these species differences in physiology and ion channel function in order to facilitate correct translation of these studies to humans. Detailed discussion of species differences in MVRCs and muscle physiology is outside the scope of this current review; interested readers are referred to the discussion by Suetterlin et al. (2022). However, the extension of muscle excitability studies to mice is an important development, which is anticipated to facilitate detailed studies of various potential therapeutic interventions under laboratory conditions.

7. Conclusions and future directions

Muscle excitability testing is an emerging technique that provides *in vivo* information about muscle fibre membrane properties such as membrane potential and ion channel function. Automated and fast applications, so-called multi-fibre MVRC, frequency ramp and repetitive stimulation protocols have accelerated the use of muscle excitability testing. So far, the technique has been used mainly in research for revealing disease mechanisms across a broad range of neuromuscular disorders, but it may have additional diagnostic uses; value has been shown particularly in muscle channelopathies and critical illness myopathy. Interpretation of muscle excitability testing would benefit from further animal studies and modelling, while new software is needed to make the technique more widely available.

Declaration competing of interest

Hugh Bostock and James Howells receive from UCL shares of the royalties for sales of the Qtrac software. The other authors have no potential conflicts of interest to declare.

This study has not received any funding.

Author contributions

HT, HB, SVT, JH, KN and WJZ contributed to the conception and design of the review and drafting of the text and preparing the figures and tables for individual sections corresponding to their expertise. HT and WJN contributed to drafting the final text. All authors rewieved and edited the manuscript.

References

Ackermann KA, Bostock H, Brander L, Schroder R, Djafarzadeh S, Tuchscherer D, et al. Early changes of muscle membrane properties in porcine faecal peritonitis. Crit Care 2014;18(4):484. https://doi.org/10.1186/s13054-014-0484-2.

Allen DC, Arunachalam R, Mills KR. Critical illness myopathy: further evidence from muscle-fiber excitability studies of an acquired channelopathy. Muscle Nerve 2008;37(1):14–22. https://doi.org/10.1002/mus.20884.

Aquilonius SM, Askmark H, Gillberg PG, Nandedkar S, Olsson Y, Stalberg E. Topographical localization of motor endplates in cryosections of whole human muscles. Muscle Nerve 1984;7(4):287–93. https://doi.org/10.1002/mus.880070406.

Bendahhou S, Cummins TR, Kula RW, Fu YH, Ptacek LJ. Impairment of slow inactivation as a common mechanism for periodic paralysis in DIIS4-S5. Neurology 2002;58(8):1266–72. https://doi.org/10.1212/wnl.58.8.1266.

Bendahhou S, Cummins TR, Tawil R, Waxman SG, Ptacek LJ. Activation and inactivation of the voltage-gated sodium channel: role of segment S5 revealed by a novel hyperkalaemic periodic paralysis mutation. J Neurosci 1999;19(12):4762–71. https://doi.org/10.1523/JNEUROSCI.19-12-04762.1999.

Benders AA, Wevers RA, Veerkamp JH. Ion transport in human skeletal muscle cells: disturbances in myotonic dystrophy and Brody's disease. Acta Physiol Scand 1996;156(3):355–67. https://doi.org/10.1046/j.1365-201X.1996.202000.x.

Benveniste O, Guiguet M, Freebody J, Dubourg O, Squier W, Maisonobe T, et al. Long-term observational study of sporadic inclusion body myositis. Brain 2011;134(Pt 11):3176–84. https://doi.org/10.1093/brain/awr213.

Beránek R. Intracellular stimulation myography in man. Electroencephalogr Clin Neurophysiol 1964;16:301–4. https://doi.org/10.1016/0013-4694(64)90114-2.

Boerio D, Correa TD, Jakob SM, Ackermann KA, Bostock H, Z'Graggen WJ. Muscle membrane properties in A pig sepsis model: Effect of norepinephrine. Muscle Nerve 2018;57(5):808–13. https://doi.org/10.1002/mus.26013.

Boerio D, Lefaucheur JP, Bassez G, Hogrel JY. Central and peripheral components of exercise-related fatigability in myotonic dystrophy type 1. Acta Neurol. Scand 2012a;125(1):38–46. http://www.ncbi.nlm.nih.gov/pubmed/22188374.

Boerio D, Z'Graggen WJ, Tan SV, Guetg A, Ackermann K, Bostock H. Muscle velocity recovery cycles: effects of repetitive stimulation on two muscles. Muscle Nerve 2012b;46(1):102–11. http://www.ncbi.nlm.nih.gov/pubmed/22692998.

Boland-Freitas R, Lee J, Howells J, Liang C, Corbett A, Nicholson G, Ng K. Sarcolemmal excitability in the myotonic dystrophies. Muscle Nerve 2018;57(4):595–602. https://doi.org/10.1002/mus.25962.
Boland-Freitas R, Lee JH, Ng K. Serum electrolyte concentrations and skeletal muscle excitability in vivo. Clin Neurophysiol 2022;135:13–21. https://doi.org/10.1016/j.clinph.2021.12.008.
Boncompagni S, Moussa CE, Levy E, Pezone MJ, Lopez JR, Protasi F, et al. Mitochondrial dysfunction in skeletal muscle of amyloid precursor protein-overexpressing mice. J Biol Chem 2012;287(24):20534–44. https://doi.org/10.1074/jbc.M112.359588.
Bostock H, Baumann C, Humm AM, Z'Graggen WJ. Temperature dependency of human muscle velocity recovery cycles. Muscle Nerve 2012a;46(2):264–6. http://www.ncbi.nlm.nih.gov/pubmed/22806376.
Bostock H, Tan SV, Boerio D, Z'Graggen WJ. Validity of multi-fiber muscle velocity recovery cycles recorded at a single site using submaximal stimuli. Clin. Neurophysiol 2012b;123(11):2296–305. http://www.ncbi.nlm.nih.gov/pubmed/22608475.
Buchanan R, Nielsen OB, Clausen T. Excitation- and beta(2)-agonist-induced activation of the Na(+)-K(+) pump in rat soleus muscle. J Physiol 2002;545(1):229–40. https://doi.org/10.1113/jphysiol.2002.023325.
Campistol JM. Uremic myopathy. Kidney Int 2002;62(5):1901–13. https://doi.org/10.1046/j.1523-1755.2002.00614.x.
Cannon SC, Strittmatter SM. Functional expression of sodium channel mutations identified in families with periodic paralysis. Neuron 1993;10(2):317–26. https://doi.org/10.1016/0896-6273(93)90321-h.
Chen W, Wang Y, Abe Y, Cheney L, Udd B, Li YP. Haploinsuffciency for Znf9 in Znf9 +/- mice is associated with multiorgan abnormalities resembling myotonic dystrophy. J Mol Biol 2007;368(1):8–17. https://doi.org/10.1016/j.jmb.2007.01.088.
Cunningham Jr JN, Carter NW, Rector Jr FC, Seldin DW. Resting transmembrane potential difference of skeletal muscle in normal subjects and severely ill patients. J Clin Invest 1971;50(1):49–59. https://doi.org/10.1172/JCI106483.
Denslow JS, Hassett CC. The polyphasic action currents of the motor unit complex. Am J Physiol-Legacy Content 1943;139(4):652–60. https://doi.org/10.1152/ajplegacy.1943.139.4.652.
DiFranco M, Herrera A, Vergara JL. Chloride currents from the transverse tubular system in adult mammalian skeletal muscle fibers. J Gen Physiol 2011;137(1):21–41. https://doi.org/10.1085/jgp.201010496.
Fournier E, Viala K, Gervais H, Sternberg D, Arzel-Hezode M, Laforet P, et al. Cold extends electromyography distinction between ion channel mutations causing myotonia. Ann Neurol 2006;60(3):356–65. https://doi.org/10.1002/ana.20905.
Haeseler G, Foadi N, Wiegand E, Ahrens J, Krampfl K, Dengler R, et al. Endotoxin reduces availability of voltage-gated human skeletal muscle sodium channels at depolarized membrane potentials. Crit Care Med. 2008;36(4):1239–47. https://doi.org/10.1097/CCM.0b013e31816a02cf. PMID: 18379251.
Hawash AA, Voss AA, Rich MM. Inhibiting persistent inward sodium currents prevents myotonia. Ann Neurol 2017;82(3):385–95. https://doi.org/10.1002/ana.25017.
Hayward LJ, Brown Jr RH, Cannon SC. Inactivation defects caused by myotonia-associated mutations in the sodium channel III-IV linker. J Gen Physiol 1996;107(5):559–76. https://doi.org/10.1085/jgp.107.5.559.
Hayward LJ, Sandoval GM, Cannon SC. Defective slow inactivation of sodium channels contributes to familial periodic paralysis. Neurology 1999;52(7):1447–53. https://doi.org/10.1212/wnl.52.7.1447.
Hochstrasser A, Rodriguez B, Soll N, Bostock H, Z'Graggen WJ. Effect of intermittent high-frequency stimulation on muscle velocity recovery cycle recordings. J Neurophysiol 2021;126(3):736–42. https://doi.org/10.1152/jn.00213.2021.
Humm AM, Bostock H, Troller R, Z'Graggen WJ. Muscle ischaemia in patients with orthostatic hypotension assessed by velocity recovery cycles. J. Neurol. Neurosurg. Psychiatry 2011;82(12):1394–8. http://www.ncbi.nlm.nih.gov/pubmed/21653205.
Jacobs AE, Benders AA, Oosterhof A, Veerkamp JH, van Mier P, Wevers RA, et al. The calcium homeostasis and the membrane potential of cultured muscle cells from patients with myotonic dystrophy. Biochim Biophys Acta 1990;1096(1):14–9. https://doi.org/10.1016/0925-4439(90)90006-b.
Kiernan MC, Bostock H, Park SB, Kaji R, Krarup C, Krishnan AV, et al. Measurement of axonal excitability: Consensus guidelines. Clin Neurophysiol 2020;131(1):308–23. https://doi.org/10.1016/j.clinph.2019.07.023.
Kristensen AG, Khan KS, Bostock H, Khan BS, Gylfadottir S, Andersen H, et al. MScanFit motor unit number estimation and muscle velocity recovery cycle recordings in diabetic polyneuropathy. Clin Neurophysiol 2020;131(11):2591–9. https://doi.org/10.1016/j.clinph.2020.07.017.
Kristensen RS, Bostock H, Tan SV, Witt A, Fuglsang-Frederiksen A, Qerama E, et al. MScanFit motor unit number estimation (MScan) and muscle velocity recovery cycle recordings in amyotrophic lateral sclerosis patients. Clin Neurophysiol 2019;130(8):1280–8. https://doi.org/10.1016/j.clinph.2019.04.713.
Larsen LH, Z'Graggen WJ, Bostock H, Tan SV, Buus NH, Tankisi H. The role of potassium in muscle membrane dysfunction in end-stage renal disease. Clin Neurophysiol 2021;132(12):3125–35. https://doi.org/10.1016/j.clinph.2021.09.012.
Lee JH, Boland-Freitas R, Liang C, Ng K. Sarcolemmal depolarization in sporadic inclusion body myositis assessed with muscle velocity recovery cycles. Clin Neurophysiol 2019a;130(12):2272–81. https://doi.org/10.1016/j.clinph.2019.08.019.
Lee JHF, Boland-Freitas R, Ng K. Sarcolemmal excitability changes in normal human aging. Muscle Nerve 2018;57(6):981–8. https://doi.org/10.1002/mus.26058.
Lee JHF, Boland-Freitas R, Ng K. Physiological differences in sarcolemmal excitability between human muscles. Muscle Nerve 2019b;60(4):433–6. https://doi.org/10.1002/mus.26645.
Meldgaard M, Kristensen RS, Z'Graggen WJ, Tan SV, Sondergaard K, Qerama E, et al. Muscle velocity recovery cycles in myopathy. Clin Neurophysiol 2023;151:41–9. https://doi.org/10.1016/j.clinph.2023.04.001.
Mihelin M, Trontelj JV, Stålberg E. Muscle fiber recovery functions studied with double pulse stimulation. Muscle Nerve 1991;14(8):739–47. https://doi.org/10.1002/mus.880140808.
Mitrovic N, George Jr AL, Heine R, Wagner S, Pika U, Hartlaub U, et al. K(+)-aggravated myotonia: destabilization of the inactivated state of the human muscle Na+ channel by the V1589M mutation. J Physiol 1994;478(Pt 3):395–402. https://doi.org/10.1113/jphysiol.1994.sp020260.
Mounsey JP, Xu P, John 3rd JE, Horne LT, Gilbert J, Roses AD, et al. Modulation of skeletal muscle sodium channels by human myotonin protein kinase. J Clin Invest 1995;95(5):2379–84. https://doi.org/10.1172/JCI117931.
Mukhamedyarov MA, Volkov EM, Khaliullina DF, Grigoryev PN, Zefirov AL, Palotas A. Impaired electro-genesis in skeletal muscle fibers of transgenic Alzheimer mice. Neurochem Int 2014;64:24–8. https://doi.org/10.1016/j.neuint.2013.10.014.
Myers JH, Denman K, DuPont C, Hawash AA, Novak KR, Koesters A, et al. The mechanism underlying transient weakness in myotonia congenita. Elife 2021;10. https://doi.org/10.7554/eLife.65691.
Needham M, Mastaglia FL. Sporadic inclusion body myositis: A review of recent clinical advances and current approaches to diagnosis and treatment. Clin Neurophysiol 2016;127(3):1764–73. https://doi.org/10.1016/j.clinph.2015.12.011.
Pedersen TH, de Paoli FV, Flatman JA, Nielsen OB. Regulation of ClC-1 and KATP channels in action potential-firing fast-twitch muscle fibers. J Gen Physiol 2009;134(4):309–22. https://doi.org/10.1085/jgp.200910290.
Riisager A, de Paoli FV, Yu WP, Pedersen TH, Chen TY, Nielsen OB. Protein kinase C-dependent regulation of ClC-1 channels in active human muscle and its effect on fast and slow gating. J Physiol 2016;594(12):3391–406. https://doi.org/10.1113/JP271556.
Rodriguez B, Branca M, Gutt-Will M, Roth M, Soll N, Nansoz S, et al. Development and early diagnosis of critical illness myopathy in COVID-19 associated acute respiratory distress syndrome. J Cachexia Sarcopenia Muscle 2022;13(3):1883–95. https://doi.org/10.1002/jcsm.12989.
Rodriguez B, Jost K, Larsen LH, Tankisi H, Z'Graggen WJ. Leg pain in neuropathic postural tachycardia syndrome is associated with altered muscle membrane properties. Clin Auton Res 2021;31(6):719–27. https://doi.org/10.1007/s10286-021-00830-5.
Rojas CV, Neely A, Velasco-Loyden G, Palma V, Kukuljan M. Hyperkalemic periodic paralysis M1592V mutation modifies activation in human skeletal muscle Na+ channel. Am J Physiol 1999;276(1):C259–66. https://doi.org/10.1152/ajpcell.1999.276.1.C259.
Ruijs TQ, Koopmans IW, de Kam ML, Tannemaat MR, Groeneveld GJ, Heuberger J. Muscle velocity recovery cycles as pharmacodynamic biomarker: Effects of mexiletine in a randomized double-blind placebo-controlled cross-over study. Clin Transl Sci 2022;15(12):2971–81. https://doi.org/10.1111/cts.13418.
Shattock MJ. Phospholemman: its role in normal cardiac physiology and potential as a druggable target in disease. Curr Opin Pharmacol 2009;9(2):160–6. https://doi.org/10.1016/j.coph.2008.12.015.
Sinha AD, Agarwal R. Chronic renal disease progression: treatment strategies and potassium intake. Semin Nephrol 2013;33(3):290–9. https://doi.org/10.1016/j.semnephrol.2013.04.009.
Stålberg E. Propagation velocity in human muscle fibers in situ. Acta Physiol Scand Suppl 1966;287:1–112. https://www.ncbi.nlm.nih.gov/pubmed/5958263.
Suetterlin KJ, Mannikko R, Matthews E, Greensmith L, Hanna MG, Bostock H, et al. Excitability properties of mouse and human skeletal muscle fibres compared by muscle velocity recovery cycles. Neuromuscul Disord 2022;32(4):347–57. https://doi.org/10.1016/j.nmd.2022.02.011.
Suetterlin KJ, Tan SV, Mannikko R, Phadke R, Orford M, Eaton S, et al. Ageing contributes to phenotype transition in a mouse model of periodic paralysis. JCSM Rapid Commun 2021;4(2):245–59. https://doi.org/10.1002/rco2.41.
Tan SV, Matthews E, Barber M, Burge JA, Rajakulendran S, Fialho D, et al. Refined exercise testing can aid DNA-based diagnosis in muscle channelopathies. Ann Neurol 2011;69(2):328–40. https://doi.org/10.1002/ana.22238.
Tan SV, Suetterlin K, Mannikko R, Matthews E, Hanna MG, Bostock H. In vivo assessment of interictal sarcolemmal membrane properties in hypokalaemic and hyperkalaemic periodic paralysis. Clin Neurophysiol 2020;131(4):816–27. https://doi.org/10.1016/j.clinph.2019.12.414.
Tan SV, Z'Graggen WJ, Boerio D, Turner C, Hanna MG, Bostock H. In vivo assessment of muscle membrane properties in myotonic dystrophy. Muscle Nerve 2016;54(2):249–57. https://doi.org/10.1002/mus.25025.
Tan SV, Z'Graggen WJ, Boerio D, Rayan DL, Howard R, Hanna MG, et al. Membrane dysfunction in Andersen-Tawil syndrome assessed by velocity recovery cycles.

Muscle Nerve 2012;46(2):193–203. http://www.ncbi.nlm.nih.gov/pubmed/22806368.

Tan SV, Z'Graggen WJ, Boerio D, Rayan DR, Norwood F, Ruddy D, et al. Chloride channels in myotonia congenita assessed by velocity recovery cycles. Muscle Nerve 2014;49(6):845–57. http://www.ncbi.nlm.nih.gov/pubmed/24037712.

Tan SV, Z'Graggen WJ, Hanna MG, Bostock H. In vivo assessment of muscle membrane properties in the sodium channel myotonias. Muscle Nerve 2018;57(4):586–94. https://doi.org/10.1002/mus.25956.

Tankisi A, Pedersen TH, Bostock H, Z'Graggen WJ, Larsen LH, Meldgaard M, et al. Early detection of evolving critical illness myopathy with muscle velocity recovery cycles. Clin Neurophysiol 2021;132(6):1347–57. https://doi.org/10.1016/j.clinph.2021.01.017.

Tankisi H, Bostock H, Grafe P. A test to determine the site of abnormal neuromuscular refractoriness. Clin Neurophysiol Pract 2022;7:1–6. https://doi.org/10.1016/j.cnp.2021.11.001.

Thor MG, Vivekanandam V, Sampedro-Castaneda M, Tan SV, Suetterlin K, Sud R, et al. Myotonia in a patient with a mutation in an S4 arginine residue associated with hypokalaemic periodic paralysis and a concomitant synonymous CLCN1 mutation. Sci Rep 2019;9(1):17560. https://doi.org/10.1038/s41598-019-54041-0.

Witt A, Bostock H, Z'Graggen WJ, Tan SV, Kristensen AG, Kristensen RS, et al. Muscle velocity recovery cycles to examine muscle membrane properties. J Vis Exp 2020a;156. https://doi.org/10.3791/60788.

Witt A, Fuglsang-Frederiksen A, Finnerup NB, Kasch H, Tankisi H. Detecting peripheral motor nervous system involvement in chronic spinal cord injury using two novel methods: MScanFit MUNE and muscle velocity recovery cycles. Clin Neurophysiol 2020b;131(10):2383–92. https://doi.org/10.1016/j.clinph.2020.06.032.

Witt A, Kristensen RS, Fuglsang-Frederiksen A, Pedersen TH, Finnerup NB, Kasch H, et al. Muscle velocity recovery cycles in neurogenic muscles. Clin Neurophysiol 2019;130(9):1520–7. https://doi.org/10.1016/j.clinph.2019.05.030.

Yang N, Ji S, Zhou M, Ptacek LJ, Barchi RL, Horn R, et al. Sodium channel mutations in paramyotonia congenita exhibit similar biophysical phenotypes in vitro. Proc Natl Acad Sci U S A 1994;91(26):12785–9. https://doi.org/10.1073/pnas.91.26.12785.

Z'Graggen WJ, Trautmann JP, Boerio D, Bostock H. Muscle velocity recovery cycles: Comparison between surface and needle recordings. Muscle Nerve 2016a;53(2):205–8. https://doi.org/10.1002/mus.24726.

Z'Graggen WJ, Aregger F, Farese S, Humm AM, Baumann C, Uehlinger DE, et al. Velocity recovery cycles of human muscle action potentials in chronic renal failure. Clin. Neurophysiol 2010;121(6):874–81. http://www.ncbi.nlm.nih.gov/pubmed/20181515.

Z'Graggen WJ, Bostock H. Velocity recovery cycles of human muscle action potentials and their sensitivity to ischemia. Muscle Nerve 2009;39(5):616–26. http://www.ncbi.nlm.nih.gov/pubmed/19229874.

Z'Graggen WJ, Brander L, Tuchscherer D, Scheidegger O, Takala J, Bostock H. Muscle membrane dysfunction in critical illness myopathy assessed by velocity recovery cycles. Clin. Neurophysiol 2011a;122(4):834–41. http://www.ncbi.nlm.nih.gov/pubmed/21044861.

Z'Graggen WJ, Tankisi H. Critical illness myopathy. J Clin Neurophysiol 2020;37(3):200–4. https://doi.org/10.1097/WNP.0000000000000652.

Z'Graggen WJ, Trautmann JP, Bostock H. Force training induces changes in human muscle membrane properties. Muscle Nerve 2016b;54(1):144–6. https://doi.org/10.1002/mus.25149.

Z'Graggen WJ, Troller R, Ackermann KA, Humm AM, Bostock H. Velocity recovery cycles of human muscle action potentials: repeatability and variability. Clin. Neurophysiol 2011b;122(11):2294–9. http://www.ncbi.nlm.nih.gov/pubmed/21555240.

Z'Graggen WJ, Lin CS, Howard RS, Beale RJ, Bostock H. Nerve excitability changes in critical illness polyneuropathy. Brain. 2006;129(Pt 9):2461–70. https://doi.org/10.1093/brain/awl191. Epub 2006 Aug 10. PMID: 16901913.

Zeppelin Z, Vaeggemose M, Witt A, Hvid LG, Tankisi H. Exploring the peripheral mechanisms of lower limb immobilisation on muscle function using novel electrophysiological methods. Clin Neurophysiol 2023;151:18–27. https://doi.org/10.1016/j.clinph.2023.04.002.